2. Barrera, J.M. *et al.* Persistent hepatitis C viremia after acute self-limiting posttransfusion hepatitis C. *Hepatology* **21**, 639–644 (1995).
3. Welzel, T.M. *et al.* Variants in interferon-alpha pathway genes and response to pegylated interferon-Alpha2a plus ribavirin for treatment of chronic hepatitis C virus infection in the hepatitis C antiviral long-term treatment against cirrhosis trial. *Hepatology* **49**, 1847–1858 (2009).
4. Yoshida, H. *et al.* Interferon therapy reduces the risk for hepatocellular carcinoma. *Ann. Intern. Med.* **131**, 174–181 (1999).
5. Kiyosawa, K. *et al.* Hepatocellular carcinoma: recent trends in Japan. *Gastroenterology* **127**, S17–S26 (2004).
6. Taura, N. *et al.* Aging of patients with hepatitis C virus-associated hepatocellular carcinoma: long-term trends in Japan. *Oncol. Rep.* **16**, 837–843 (2006).
7. Miki, D. *et al.* Clinicopathological features of elderly patients with hepatitis C virus-related hepatocellular carcinoma. *J. Gastroenterol.* **43**, 550–557 (2008).
8. Takata, A. *et al.* HCC develops even in the early stage of chronic liver disease in elderly patients with HCV infection. *Int. J. Mol. Med.* **26**, 249–256 (2010).
9. Yuen, M.F., Hou, J.L. & Chutaputti, A. Hepatocellular carcinoma in the Asia pacific region. *J. Gastroenterol. Hepatol.* **24**, 346–353 (2009).
10. Manns, M.P. *et al.* Peginterferon alfa-2b plus ribavirin compared with interferon alfa-2b plus ribavirin for initial treatment of chronic hepatitis C: a randomised trial. *Lancet* **358**, 958–965 (2001).
11. Zhang, H. *et al.* Genome-wide association study identifies 1p36.22 as a new susceptibility locus for hepatocellular carcinoma in chronic hepatitis B virus carriers. *Nat. Genet.* **42**, 755–758 (2010).
12. Ura, S. *et al.* Differential microRNA expression between hepatitis B and hepatitis C leading disease progression to hepatocellular carcinoma. *Hepatology* **49**, 1098–1112 (2009).
13. Pe'er, I., Yelensky, R., Altshuler, D. & Daly, M.J. Estimation of the multiple testing burden for genomewide association studies of nearly all common variants. *Genet. Epidemiol.* **32**, 381–385 (2008).
14. Yamauchi, T. *et al.* A genome-wide association study in the Japanese population identifies susceptibility loci for type 2 diabetes at UBE2E2 and C2CD4A–C2CD4B. *Nat. Genet.* **42**, 864–868 (2010).
15. Ono, E. *et al.* Platelet count reflects stage of chronic hepatitis C. *Hepatol. Res.* **15**, 192–200 (1999).
16. Poynard, T. & Bedossa, P. Age and platelet count: a simple index for predicting the presence of histological lesions in patients with antibodies to hepatitis C virus. *J. Viral Hepat.* **4**, 199–208 (1997).
17. Forns, X. *et al.* Identification of chronic hepatitis C patients without hepatic fibrosis by a simple predictive model. *Hepatology* **36**, 986–992 (2002).
18. Wai, C.T. *et al.* A simple noninvasive index can predict both significant fibrosis and cirrhosis in patients with chronic hepatitis C. *Hepatology* **38**, 518–526 (2003).
19. Pohl, A. *et al.* Serum aminotransferase levels and platelet counts as predictors of degree of fibrosis in chronic hepatitis C virus infection. *Am. J. Gastroenterol.* **96**, 3142–3146 (2001).
20. Seng, T.J. *et al.* Complex chromosome 22 rearrangements in astrocytic tumors identified using microsatellite and chromosome 22 tile path array analysis. *Genes Chromosom. Cancer* **43**, 181–193 (2005).
21. Kharrat, A. *et al.* Conformational stability studies of the pleckstrin DEP domain: definition of the domain boundaries. *Biochim. Biophys. Acta* **1385**, 157–164 (1998).
22. Harada, Y. *et al.* Cell-permeable peptide DEPDC1–ZNF224 interferes with transcriptional repression and oncogenicity in bladder cancer cells. *Cancer Res.* **70**, 5829–5839 (2010).
23. Kanehira, M. *et al.* Involvement of upregulation of DEPDC1 (DEP domain containing 1) in bladder carcinogenesis. *Oncogene* **26**, 6448–6455 (2007).

ONLINE METHODS

Samples. We conducted a two-phase case control study consisting of GWAS and replication phases using 3,312 Japanese subjects over the age of 55 with chronic HCV infection diagnosed at Toranomon Hospital Department of Hepatology (n = 727), Sapporo Kosei Hospital (n = 153) and Hiroshima University–affiliated hospitals (n = 2,432) between 2002 and 2010. Individuals with chronic HCV with HCC were enrolled as cases, and those without were enrolled as controls. Cases and controls were then each randomly divided into two sets, totaling 212 cases and 765 controls in the GWAS phase and 710 cases and 1,625 controls in the replication phase. All subjects had abnormal levels of serum alanine transaminase for more than 6 months and were positive for both HCV antibody and serum HCV RNA. All subjects were negative for hepatitis B surface antigen, had no evidence of other liver diseases and had not received immunosuppressive therapy before enrollment in the study. Clinical information such as age, gender and platelet count were available in all subjects. For cases, age and platelet count at initial diagnosis of HCC were used. The subject characteristics are shown in **Supplementary Table 10**. The diagnosis of HCC was based on hypervascularity confirmed by dynamic computed tomography, magnetic resonance imaging, angiography or computed tomography angiography when the serum levels of HCC-related tumor markers, such as alpha fetoprotein or protein induced in the absence of vitamin K or antagonist II (PIVKA-II), were increased or a mass lesion was detected by ultrasonography. When a nodule was not proven to be hypervascular, percutaneous biopsy under ultrasonography was performed for confirmation of the diagnosis of HCC. Staging of HCC adopted in this study was the revised version of Liver Cancer Study Group of Japan[24]. The average quantity of alcohol consumed per day was evaluated regardless of alcohol beverage. Habitual alcohol intake was defined as ≥80 g/day for more than 5 years. All subjects in the present study received a detailed explanation and all signed a written informed consent form. The study was approved by the ethical committee of each participating medical center and by the Ethical Committee at the SNP Research Center, the Institute of Physical and Chemical Research (RIKEN), Yokohama, Japan.

SNP genotyping. Genomic DNA was extracted from peripheral blood leukocytes using a standard method. For the GWAS stage, we genotyped 981 Japanese subjects with chronic HCV infection using the Illumina HumanHap610-Quad BeadChip. We excluded two samples with call rate <0.98, and two other samples suggesting kinship or sample duplication were excluded from the analysis based on PI_HAT value (>0.4). We assessed population stratification using the smartpca program in the EIGENSOFT package using SNPs informative for the Japanese population according to a previously described method[25]. Analysis was performed based on the GWAS data and the Japanese (JPT), Han-Chinese (CHB), European (CEU) and African (YRI) individuals from the HapMap project. Principal component analysis identified no outliers from the JPT/CHB clusters. In total, 467,538 autosomal SNPs passed the quality control filters (call rate ≥ 0.99 in both cases and controls, MAF ≥ 0.01 and a Hardy-Weinberg equilibrium $P \geq 1.0 \times 10^{-6}$ in controls). We used multiplex-PCR–based Invader assays (Third Wave Technologies) for the replication study (710 cases and 1,625 controls) and fine mapping[26]. Samples for both cases and controls were distributed randomly on genotyping plates in both phases of the study, and all persons performing genotyping and interpretation of results were blind to case or control status.

Fine mapping and resequencing. We performed fine mapping using all GWAS-stage case and control samples. Haploview was used to select tag SNPs with a pairwise $r^2 > 0.80$ and MAF ≥ 0.05 on the basis of Phase II HapMap JPT data. Resequencing of candidate regions was performed by direct sequencing of DNA from 48 unrelated Japanese individuals with HCV from among the enrolled subjects.

Quantitative analysis of mRNA of *DEPDC5*. A total of 43 paired primary hepatocellular carcinomas and adjacent non-tumor tissues, derived from 43 unrelated HCC cases enrolled, were examined. Total RNA was extracted from liver tissues using the RNeasy Mini Kit (QIAGEN). One microgram of each RNA sample was reverse transcribed with ReverseTra Ace (TOYOBO Co. Ltd.) and Random Primer (Takara Bio). We quantified the mRNA for *DEPDC5* with the SsoFast EvaGreen Supermix (Bio-Rad Laboratories). Primers were designed for the conserved region between isoforms 1 and 2 (**Supplementary Table 12**). Amplification and detection were performed using a CFX Real-Time PCR Detection System (Bio-Rad Laboratories). Results were normalized to the transcript levels of beta-actin (*ACTB*).

Statistical analysis. Genotype-based associations were tested using a Cochran-Armitage trend test[27,28]. The OR and 95% CI were calculated from a two-by-two allele frequency table. In the GWAS stage, significance levels after Bonferroni correction for multiple testing were $P = 1.07 \times 10^{-7}$ (calculated as 0.05/467,538)[13,14]. Combined analysis was performed following the Mantel-Haenszel method. Heterogeneity among studies was examined using the Breslow-Day test. We used Haploview software to analyze the association of haplotypes and LD values between *DEPDC5* and SNPs. Power analysis was performed using Power for Genetic Association Analyses software[29]. The Mann-Whitney U test was used to analyze continuous variables, and χ^2 or Fisher exact tests were used to analyze categorical data, as appropriate.

Software. For general statistical analysis, we used the R statistical environment version 2.12.0 or PLINK 1.03 (ref. 30). To draw the LD map and analyze the association of haplotypes, we used Haploview software[31].

24. The general rules for the clinical and pathological study of primary liver cancer. *Liver Cancer Study Group of Japan* 3rd English edn. (Kanehara & Co., Ltd., Tokyo, Japan, 2010).
25. Yamaguchi-Kabata, Y. *et al.* Japanese population structure, based on SNP genotypes from 7003 individuals compared to other ethnic groups: effects on population-based association studies. *Am. J. Hum. Genet.* **83**, 445–456 (2008).
26. Ohnishi, Y. *et al.* A high throughput SNP typing system for genome-wide association studies. *J. Hum. Genet.* **46**, 471–477 (2001).
27. Nam, J.M. A simple approximation for calculating sample sizes for detecting linear trend in proportions. *Biometrics* **43**, 701–705 (1987).
28. Margolin, B.H. Test for trend in proportions. in *Encyclopedia of statistical sciences.* (eds. Klotz, S. & Johnson, N.L.) 334–336 (John Wiley & Sons, Inc., New York, New York, USA, 1988).
29. Menashe, I., Rosenberg, P.S. & Chen, B.E. PGA: Power calculator for case-control genetic association analyses. *BMC Genet.* **9**, 36 (2008).
30. Purcell, S. *et al.* PLINK: a tool set for whole-genome association and population-based linkage analyses. *Am. J. Hum. Genet.* **81**, 559–575 (2007).
31. Barrett, J.C., Fry, B., Maller, J. & Daly, M.J. Haploview: analysis and visualization of LD and haplotype maps. *Bioinformatics* **21**, 263–265 (2005).

UICC
global cancer control

IJC
International Journal of Cancer

Identification of a secretory protein c19orf10 activated in hepatocellular carcinoma

Hajime Sunagozaka, Masao Honda, Taro Yamashita, Ryuhei Nishino, Hajime Takatori, Kuniaki Arai, Tatsuya Yamashita, Yoshio Sakai and Shuichi Kaneko

Department of Gastroenterology, Kanazawa University Hospital, Kanazawa, Ishikawa, Japan

The identification of genes involved in tumor growth is crucial for the development of inventive anticancer treatments. Here, we have cloned a 17-kDa secretory protein encoded by *c19orf10* from hepatocellular carcinoma (HCC) serial analysis of gene expression libraries. Gene expression analysis indicated that *c19orf10* was overexpressed in approximately two-thirds of HCC tissues compared to the adjacent noncancerous liver tissues, and its expression was significantly positively correlated with that of alpha-fetoprotein (AFP). Overexpression of *c19orf10* enhanced cell proliferation of AFP-negative HLE cells, whereas knockdown of *c19orf10* inhibited cell proliferation of AFP-positive Hep3B and HuH7 cells along with G1 cell cycle arrest. Supplementation of recombinant c19orf10 protein in culture media enhanced cell proliferation in HLE cells, and this effect was abolished by the addition of antibodies developed against c19orf10. Intriguingly, c19orf10 could regulate cell proliferation through the activation of Akt/mitogen-activated protein kinase pathways. Taken together, these data suggest that c19orf10 might be one of the growth factors and potential molecular targets activated in HCC.

Hepatocellular carcinoma (HCC) is one of the most common cancers with an estimated worldwide incidence of 1,000,000 cases per year.[1] Most HCCs develop as a consequence of chronic liver disease such as chronic viral hepatitis due to hepatitis C virus (HCV) or hepatitis B virus (HBV) infection.[2–7] Liver cirrhosis patients with any etiology are considered to be at an extremely high risk for HCC.[8–10] Indeed, ~7% of liver cirrhosis patients with HCV infection develop HCC annually,[8,11] and the advancement of reliable HCC screening methods for high-risk patients is crucial for the improvement of their overall survival.[12]

Currently, imaging diagnostic techniques such as ultrasonography, computed tomography, magnetic resonance image and angiography are the gold standards for the early detection of HCC.[13,14] In addition, tumor markers such as alpha-fetoprotein (AFP) and des-gamma carboxyl prothrombin (DCP) have been used for the screening of HCC,[15–18] although their sensitivity and specificity are not sufficiently high. Recently, a gene expression profiling approach shed new light on Glypican 3, a heparin sulfate proteoglycan anchored to the plasma membrane, as a potential HCC marker, and its clinical usefulness as a molecular target as well as a tumor marker is presently under investigation.[19]

There are several options available for the treatment of HCC, including surgical resection, liver transplantation, radiofrequency ablation, transcatheter arterial chemoembolization and chemotherapy, while taking the HCC stage and liver function into consideration. Recently, molecular therapy targeting the Raf kinase/vascular endothelial growth factor receptor (VEGFR) kinase inhibitor sorafenib improved the survival of patients with advanced HCC,[20,21] emphasizing the importance of deciphering the molecular pathogenesis of HCC for the development of effective treatment options.

Here, we investigated the gene expression profiles of HCC by serial analysis of gene expression (SAGE) to discover a novel gene activated in HCC.[22–25] We identified a gene, *c19orf10*, overexpressed in HCC and determined that the encoded 17-kDa protein (c19orf10) is a secretory protein. Murine *c19orf10* was originally discovered to encode a cytokine interleukin (IL)-25/stroma-derived growth factor (SF20) in 2001.[26] The gene *c19orf10* was mapped in the H2 complex region of mouse chromosome 17 between *C3* and *Ir5*, and the hypothetical protein was predicted as globular protein.[26] However, the subsequent study failed to reproduce its proliferative effect on lymphoid cells, and the paper was retracted by the authors in 2003.[26,27] Nevertheless, independent studies revealed that c19orf10 was indeed produced by synoviocytes, macrophages and adipocytes, although the function of c19orf10 remained elusive.[28,29] In our study, we identified that *c19orf10* was overexpressed in AFP-positive HCC samples. Our data imply that c19orf10 could activate the mitogen-activated protein kinase (MAPK)/Akt pathway and

Key words: hepatocellular carcinoma, serial analysis of gene expression, *c19orf10*
Additional Supporting Information may be found in the online version of this article
DOI: 10.1002/ijc.25830
History: Received 14 Mar 2010; Accepted 15 Nov 2010; Online 2 Dec 2010
Correspondence to: Shuichi Kaneko, Kanazawa University Hospital, 13-1 Takara-machi, Kanazawa, Ishikawa 920-8641, Japan,
Tel.: +81-76-265-2233, Fax: +81-76-234-4250,
E-mail: skaneko@m-kanazawa.jp

enhance cell proliferation in HCC cell lines, suggesting that c19orf10 may be a growth factor produced by tumor epithelial cells and/or stromal cells, and, therefore, would be a good target for the treatment of HCC.

Material and Methods

SAGE and HCC samples

HCC and normal liver SAGE libraries that we had constructed were reanalyzed using SAGE 2000 software. The size of each SAGE library was normalized to 300,000 transcripts per library. Monte Carlo simulation was used to select genes whose expression levels were significantly different between the two libraries. Each SAGE tag was annotated using the gene-mapping website SAGE Genie database (http://cgap.nci.nih.gov/SAGE/) and the SOURCE database (http://smd.stanford.edu/cgi-bin/source/sourceSearch) as previously described.[30] An additional 15 SAGE libraries of normal and cancerous tissues from various organs were retrieved using the National Center for Biotechnology Information SAGEmap (http://www.ncbi.nlm.nih.gov/SAGE/).

Fifteen HCC tissues (four HBV-related and 11 HCV-related) and the corresponding noncancerous liver tissues were obtained from HCC patients who received hepatectomy. Four normal liver tissues were obtained from patients undergoing surgical resection of the liver for the treatment of metastatic colon cancer. Additionally, 36 HCC tissues (17 HBV-related and 19 HCV-related) were obtained from HCC patients undergoing hepatectomy. These samples were snap frozen in liquid nitrogen immediately after resection and used for quantitative real-time detection PCR (RTD-PCR). Total RNA was extracted using a ToTALLY RNA™ kit (Ambion, Austin, TX).

The study protocol conformed to the ethical guidelines of the Declaration of Helsinki (1975) and was approved by the institutional ethical review board committee. All patients provided written informed consent for the analysis of the specimens.

Laser capture microdissection and RNA isolation

Laser capture microdissection (LCM) was performed as previously described.[31] Briefly, 20 HCV-related surgically resected HCC tissues were frozen in OCT compound (Sakura Finetech, Torrance, CA).[32] Inflammatory cells and cancerous cells in HCC tissues were separately excised by LCM using a Laser Scissors CRI-337 (Cell Robotics, Albuquerque, NM) under a microscope. Total RNA was isolated from these cells using a microRNA isolation kit (Stratagene, La Jolla, CA) in accordance with the supplied protocol, with slight modifications.[31]

Construction of C19ORF10 expression plasmid and recombinant adenovirus vector

PCR was performed on a Marathon cDNA library from Huh7 cells using the following primers: sense primers: 5′-GACCCTAGTCCAACATGGCGGCGCCC-3′ (the first PCR), 5′-ATGGCGGCGCCCAGCGGAGGGTGGAACGGC-3′ (the nested second PCR) and antisense primers: 5′-CACCGGA GATGAGAAGGTGCCACCCGC-3′ (the first PCR), 5′-CAG GGCTGCTGGTCACAGCTCAGTGCGCG-3′ (the nested second PCR). The 5′ and 3′ends of the cDNA were isolated using a SMART RACE cDNA Amplification kit (Clontech, Mountain View, CA) according to the manufacturer's recommendations. The PCR products were cloned into a TA vector (Invitrogen, Carlsbad, CA) to generate the pcDNA3.1-*c19orf10* expression plasmid. Using this plasmid, a C-terminally FLAG-tagged construct of *c19orf10* was generated and inserted in a pSI mammalian expression vector (Promega, Madison, WI), which was driven by the SV40 promoter (pSI-*c19orf10*).

The replication-incompetent recombinant adenovirus vector expressing FLAG-tagged *c19orf10* (Ad. *c19orf10-FLAG*) was generated by homologous recombination using the AdMax system (Microbix, Toronto, Canada) as previously described.[33] The generated recombinant adenovirus was purified by limiting dilution, and the titer of viral aliquots was determined by the 50% tissue culture infectious dose method as previously described.[34]

RTD-PCR

RTD-PCR was performed as previously described.[31] Briefly, template cDNA was synthesized from 1 μg of total RNA using SuperScript™ II RT (Invitrogen). RTD-PCR of *c19orf10* (Hs. 00384077_m1), *AFP* (Hs00173490_m1), *GPC3* (Hs01018938_m1), *KRT19* (Hs00761767_s1) and the *ACTB* internal control (Hs99999903_m1) was performed using a TaqMan® Gene Expression Assay kit (Applied Biosystems, Foster City, CA). The expression of selected genes was measured in triplicate by ΔΔCT method using the 7900 Sequence Detection System (Applied Biosystems).

Cell lines and transfection of plasmids

Human liver cancer cell lines HuH1, Huh7, Hep3B, HLE and HLF as well as HEK293 and NIH3T3 were cultured in Dulbecco's modified Eagle's medium (Invitrogen) supplemented with 10% heat-inactivated fetal bovine serum (Invitrogen) in 5% CO_2 at 37°C. Transfection of plasmids was performed using FuGENE™ 6 (Roche Diagnostics, Indianapolis, IN) according to the manufacturer's instruction. Briefly, 5×10^5 cells were seeded in a six-well plate 12 hr before transfection, and 3 μg of plasmid DNA was used for each transfection. All experiments were repeated at least twice.

Purification of c19orf10-FLAG fused protein and production of anti-c19orf10 antibody

Approximately 500 ml of culture supernatant obtained from HEK293 cells infected with Ad. *C19ORF10-FLAG* at a multiplicity of infection of 20 was applied to an anti-FLAG affinity gel column (Sigma-Aldrich, St. Louis, MO). The column was

Table 1. ESTs overexpressed in the HCC library

Tag sequence	*p* value	HCC	Normal liver	T/N ratio	Name	UniGene ID
TGGGCAGGTG	<0.00001	33	0	>33	Chromosome 5 open reading frame 13	Hs.483067
GCAAAATATC	<0.00001	31	2	15.5	Liver cancer-associated noncoding mRNA, partial sequence	Hs.214343
AGCCTGCAGA	0.0002	12	1	12	Chromosome 19 open reading frame 10	Hs.465645
TTGTGCACGT	0.000228	12	1	12	CDNA FLJ45284 fis, clone BRHIP3001964	Hs.514273
ACATTCTTGT	0.000042	12	0	>12	Transcribed locus, strongly similar to XP_496055.1	Hs.76704
ACAAGTACCC	0.001161	10	1	>10	Chromosome 5 open reading frame 13	Hs.483067
GAGGTGAAGG	0.000174	10	0	>10	KIAA1914	Hs.501106
GCTGGAGGAG	0.000114	10	0	>10	Transcribed locus	Hs.520115

subjected to elution by competition with FLAG peptide (5 μg/ml), and each 1 ml fraction of the eluted aliquot was collected to obtain the most concentrated c19orf10-FLAG protein in accordance with the manufacturer's protocol. The anti-c19orf10 antibodies were developed by immunizing rabbits with repeated intradermal injections of purified c19orf10-FLAG. Protein concentration was measured by the Bradford method.

Silencing gene expression by short interfering RNA

The selected short interfering RNA (siRNA) targeting *C19ORF10* (Si-*C19ORF10*; Silencer Select siRNAs s31855) and the irrelevant control sequence (Si-*Control*; Silencer Select siRNAs 4390843) was obtained from Applied Biosystems. Transfection of these siRNAs was performed using FuGENE^{TM} 6 (Roche Diagnostics) as previously described.[30] Briefly, 2×10^5 cells were seeded in a six-well plate 12 hr before transfection. A total of 100 pmol/l of siRNA duplex was used for each transfection. The experiments were performed at least twice.

Cell proliferation assay

Cell proliferation was evaluated in quadruplicate using a Cell Titer 96 MTS Assay kit (Promega). Briefly, 2×10^3 HLE or HuH7 cells were harvested in a 96-well plate 12 hr before the transfection or addition of the recombinant proteins. Transfection of siRNAs or plasmids was performed using FuGENE^{TM} 6 (Roche Diagnostics). After incubation with MTS/PMS solution at 37°C for 2 hr, the absorbance at 450 nm was measured. The experiments were performed at least twice.

Cell cycle analysis

Cells were fixed using 80% ice-cold ethanol and incubated with propidium iodide for 10 min. DNA content was analyzed using a FACS Caliber flow cytometer (BD Biosciences, San Jose, CA) counting 10,000 stained cells. The distribution of cells in each cell cycle phase was determined using FlowJo software (Tree Star, Ashland, OR).

Western blotting

Cells were lysed in radioimmunoprecipitation assay (RIPA) buffer, and the extracts were subsequently electrophoresed on sodium dodecyl sulfate–10% polyacrylamide gels and transferred onto protean nitrocellulose membranes. The blots were then incubated for 1 hr with an appropriate primary monoclonal antibody: phospho-PI3K (#4228), phospho-Akt (#4060), phospho-GSK-3β (#9323), phospho-c-Raf (#9427), phospho-MEK1/2 (#9154), phospho-p44/42 MAPK (Erk1/2) (#4370), Cdk4 (CDK4 (#2906)), Cdk6 (#3136), cyclinD1 (#2926), cyclinD3 (#2936), phospho-Rb (#9308), phospho-P53 (# 9286), phospho-cdc2 (#9111) and β-actin (#4970) (Cell Signaling Technology, Allschwil, Switzerland) and anti-FLAG antibodies (Sigma-Aldrich, St. Louis, MO). The blots were washed and exposed to peroxidase-conjugated secondary antibodies, such as anti-mouse or rabbit IgG antibodies, and visualized using the ECL^{TM} kit (Amersham Biosciences, Piscataway, NJ). All experiments were performed at least twice.

Statistical analyses

Unpaired *t*-tests and Kruskal–Wallis tests were performed on the RTD-PCR and cell proliferation data using GraphPad Prism software (www.graphpad.com).

Results

Identification of *C19ORF10* overexpression in HCC by SAGE

To comprehensively explore the candidate novel genes activated in HCC, we reanalyzed two SAGE libraries derived from HCC tissues and normal liver tissues.[30] After normalization of each SAGE library size to 300,000 tags, we compared the HCC and normal liver libraries to obtain the list of genes overexpressed in HCC. We identified 79 genes significantly overexpressed in the HCC library by more than tenfold when compared to the normal liver library (Supporting Information Table 1). Among them, we explored expressed sequence tags (ESTs) as candidates for novel HCC-related genes to identify eight unique tags corresponding to seven ESTs (Table 1). We especially focused on the EST chromosome 19 open reading frame 10 (*c19orf10*) because the

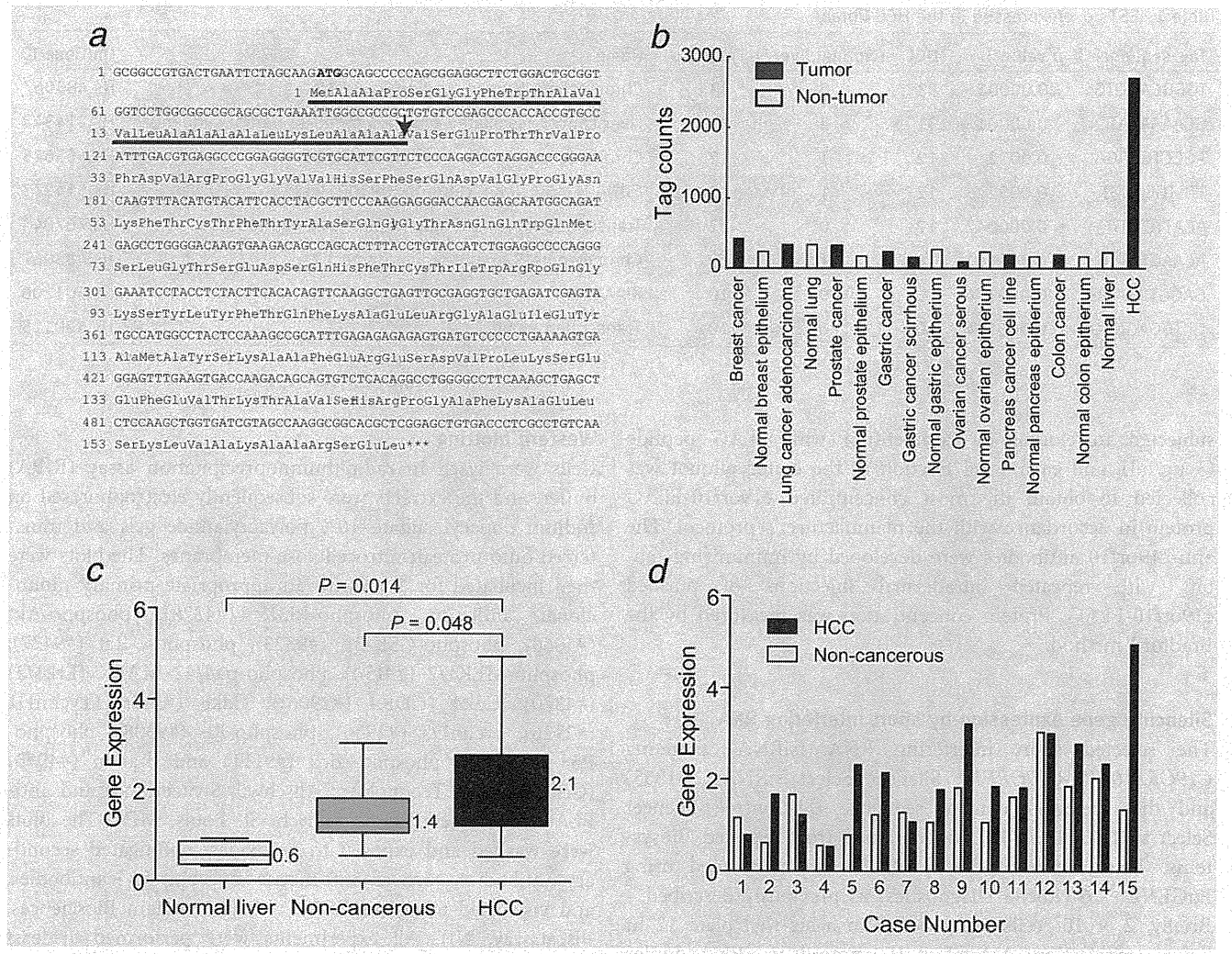

Figure 1. (*a*) Structure of a *c19orf10* gene and a c19orf10 protein. The DNA sequence of *c19orf10* and amino acid alignment of the encoded c19orf10 protein are shown. C19orf10 is predicted to have a molecular weight of 17 kDa and contain a signal peptide cleavage site (indicated as a black arrow). (*b*) *C19orf10* gene expression profiles in various tissues by SAGE. *Y*-axis indicates the number of tags corresponding to *c19orf10* in each tissue. (*c*, *d*) RTD-PCR analysis of *c19orf10*. RNA was isolated from 34 tissue samples: 15 HCC, 15 corresponding noncancerous liver samples and four normal liver samples. Differential expression of each gene among normal liver tissues, noncancerous liver tissues and HCC tissues was examined using the Kruskal–Wallis test and unpaired *t*-test. The mean value of gene expression data in each group is indicated (*c*). *C19orf10* was overexpressed in 10 of 15 examined HCC tissues compared to the noncancerous liver tissues (*d*).

sequence presumably encoded a secretory protein with a signal peptide sequence (Fig. 1*a*).

When we examined the expression profiles of *c19orf10* using retrieved SAGE data from various cancers and their normal counterparts, we identified that *c19orf10* was abundantly expressed in human HCC (Fig. 1*b*). We further examined the publicly available EST profiles of *c19orf10* (http://www.ncbi.nlm.nih.gov/unigene) and confirmed its tendency to be overexpressed in HCC compared to the normal liver (data not shown). We validated the overexpression of *c19orf10* in 15 independent HCC tissues and adjacent noncancerous liver tissues by RTD-PCR. Gene expression of *c19orf10* was significantly higher in the HCC tissues than in the normal liver tissues and adjacent noncancerous liver tissues ($p = 0.014$ and 0.048, respectively; Fig. 1*c*). *C19orf10* expression was elevated in HCC tissues compared to the adjacent noncancerous liver tissues in 10 of 15 patients (66.7%; Fig. 1*d*).

Overexpression of *C19ORF10* in AFP-positive HCC

As HCC is a heterogeneous mixture of cancer epithelial cells and stromal cells, and a previous report indicated that *c19orf10* is expressed in fibroblast-like synoviocytes. We, therefore, evaluated the expression of *c19orf10* in tumor epithelial cells and stromal cells separately using LCM and RTD-PCR in 20 HCC tissues (Fig. 2*a*). Although tumor

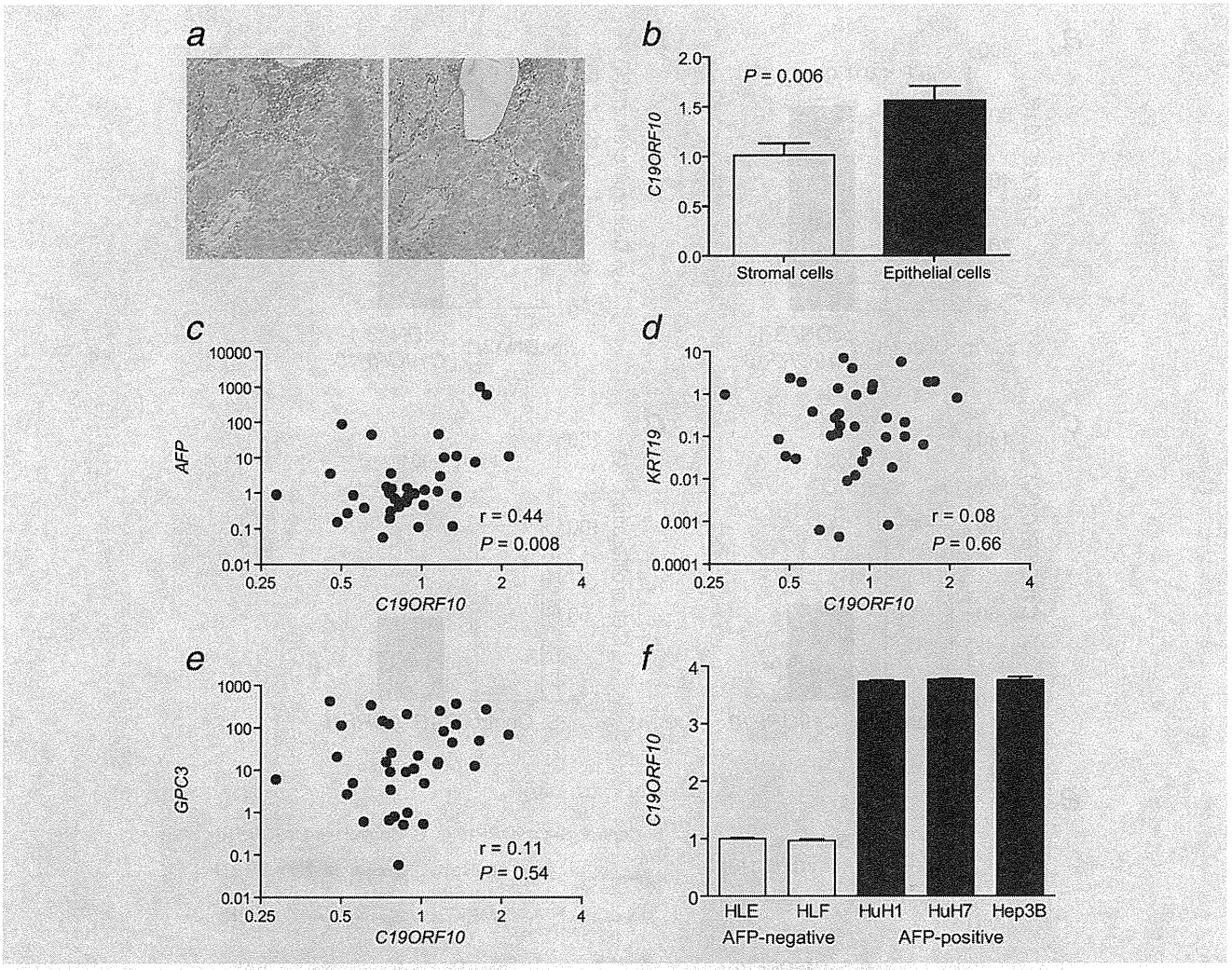

Figure 2. (*a*) Representative photomicrographs of an HCC tissue used for LCM (toluidine blue staining). Inflammatory mononuclear cells and stromal cells were separately captured (left: Pre-LCM, right: Post-LCM). (*b*) RTD-PCR analysis of *c19orf10* expression in inflammatory mononuclear cells and tumor epithelial cells in 20 HCV-related HCC tissues. Tumor-inflammatory mononuclear cells and stromal cells were isolated using LCM. RNAs were isolated from these cells as well as parenchymal tissues from the same liver, followed by RTD-PCR for *c19orf10* gene expression. Expression of the *c19orf10* gene was higher than that observed in HCC-infiltrating inflammatory mononuclear cells. *$p < 0.05$. (*c–e*) Scatter plot analysis of *c19orf10, AFP, KRT19* and *GPC3* expression in HCC. RNA was isolated from 17 HBV-related HCC and 19 HCV-related HCC. (*f*) RTD-PCR analysis of *c19orf10* in AFP-negative (HLE and HLF) and -positive (HuH1, HuH7 and Hep3B) liver cancer cell lines.

stromal cells expressed *c19orf10* at some level, the expression levels were significantly higher in tumor epithelial cells than in stromal cells ($p = 0.006$) (Fig. 2*b*).

To explore the relationship of *c19orf10* with other established HCC markers, we investigated the gene expression of *c19orf10*, *AFP* (alpha-fetoprotein), *KRT19* (cytokeratin 19) and *GPC3* (glypican 3). Because only 1 of 15 HCC tissues analyzed above (Fig. 1*d*) was AFP positive (data not shown), we further investigated the expression of *c19orf10* in an additional 36 HCC tissues using RTD-PCR. Interestingly, *c19orf10* expression was significantly positively correlated with *AFP* ($r = 0.44$, $p = 0.008$), but not with *KRT19* ($r = 0.08$, $p = 0.66$) nor *GPC3* ($r = 0.11$, $p = 0.54$) (Figs. 2*c*–2*e*). Furthermore, when we examined the expression of *c19orf10* in AFP-positive (HuH1, HuH7 and Hep3B) and -negative (HLE and HLF) HCC cell lines, we identified the overexpression of *c19orf10* in AFP-positive HCC cell lines (Fig. 2*f*). These data suggested that *c19orf10* is overexpressed and may play some role in AFP-positive HCCs.

C19orf10 regulates MAPK/Akt pathways and activates cell proliferation

To explore the functional role of c19orf10 in HCC, we performed *c19orf10* overexpression and knockdown studies using *c19orf10*-low HLE cells and *c19orf10*-high Hep3B and HuH7 cells, respectively. When we transfected HLE cells with

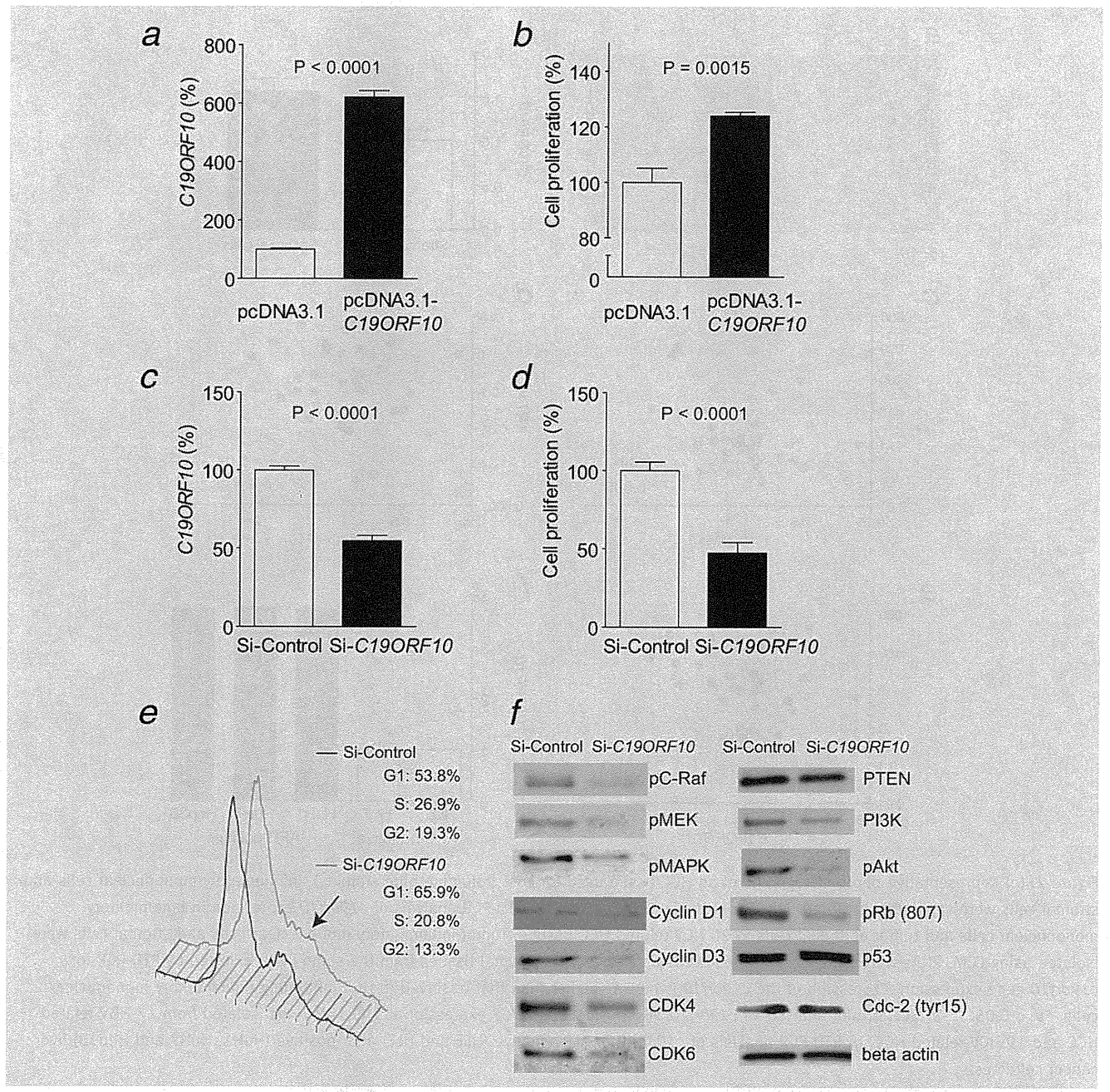

Figure 3. (*a*) RTD-PCR analysis of *c19orf10* expression in HLE cells transfected with pcDNA3.1 or pcDNA3.1-*c19orf10* plasmids. (*b*) Cell proliferation assay of HLE cells transfected with pcDNA3.1 or pcDNA3.1-*c19orf10* plasmids. Cell proliferation was evaluated 72 hr after each plasmid transfection. (*c*) RTD-PCR analysis of *c19orf10* expression in Hep3B cells transfected with Si-*Control* or Si-*c19orf10*. Gene expression was measured in triplicates 48 hr after transfection. (*d*) Cell proliferation assay of Hep3B cells transfected with Si-*Control* or Si-*c19orf10*. Cell proliferation was evaluated 72 hr after siRNA transfection. (*e*) Cell cycle analysis of HuH7 cells transfected with Si-*Control* or Si-*c19orf10*. Cell cycle was evaluated 72 hr after siRNA transfection. A black arrow indicates the G2 phase peak. (*f*) Western blotting analysis of Huh7 cells transfected with Si-*Control* or Si-*c19orf10*. Cells were lysed by RIPA buffer 72 hr after siRNA transfection.

pcDNA3.1 or pcDNA3.1-*c19orf10* plasmids, we identified an approximately sixfold overexpression of *c19orf10* when compared to the control 48 hr after transfection ($p < 0.0001$) (Fig. 3*a*). Interestingly, cell proliferation was modestly, but significantly, enhanced compared to the control 72 hr after transfection ($p = 0.0015$) (Fig. 3*b*).

We also transfected siRNAs targeting an irrelevant sequence (Si-*Control*) or *c19orf10* (Si-*c19orf10*) in Hep3B and

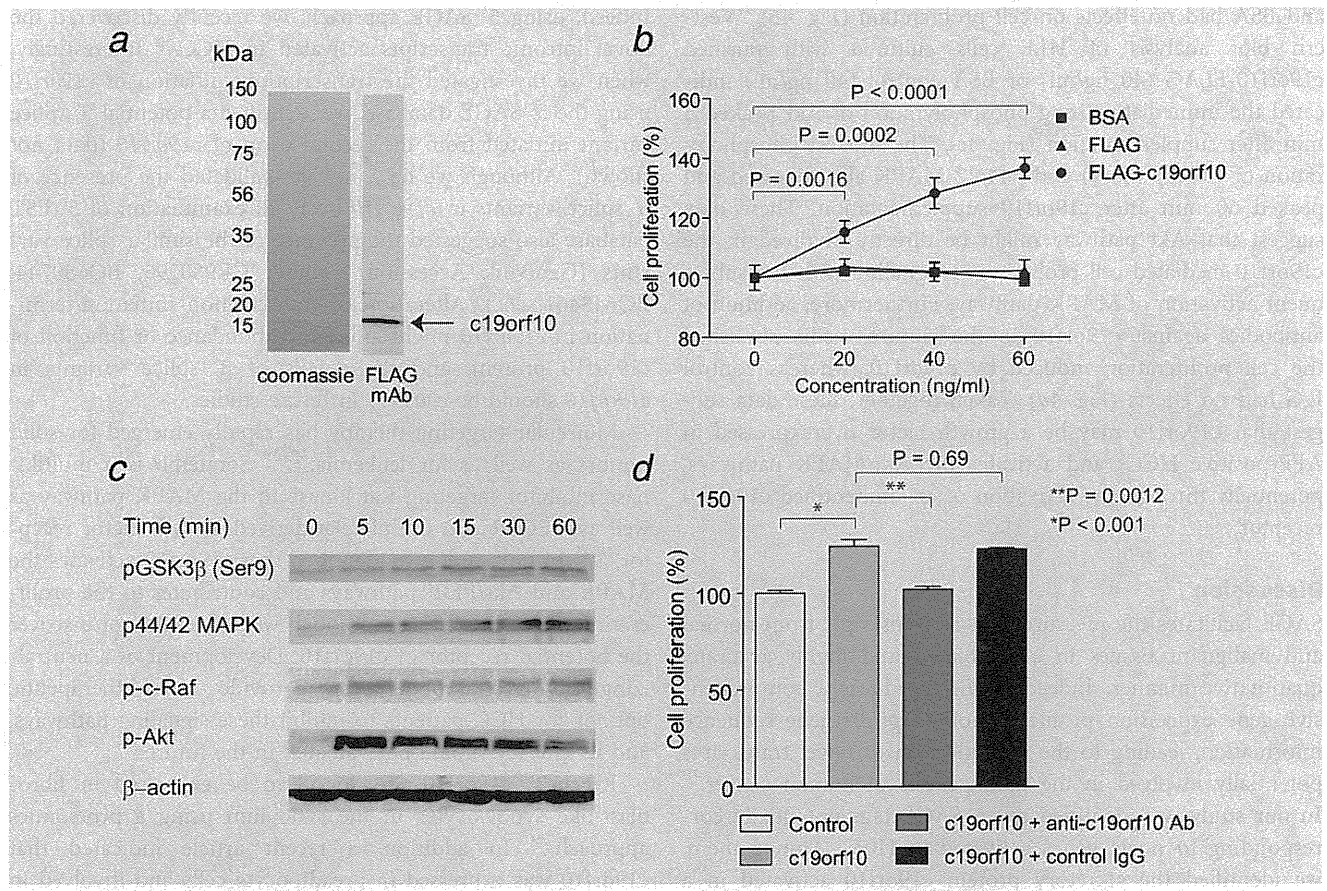

Figure 4. (*a*) Coomassie blue staining and Western blotting of culture supernatant of NIH3T3 cells transfected with pSI-*c19orf10-FLAG*. A black arrow indicates the 17-kDa c19orf10 protein. (*b*) Cell proliferation assay of HLE cells supplemented with recombinant c19orf10-FLAG, FLAG peptides or BSA. Cell proliferation was measured in quadruplicates 72 hr after supplementation. (*c*) Western blotting of HLE cells supplemented with c19orf10-FLAG (40 ng/ml). Cells were lysed at indicated time after c19orf10 supplementation. (*d*) Cell proliferation assay of HLE cells supplemented with control BSA (40 ng/ml) (white bar), c19orf10-FLAG (40 ng/ml) (light gray bar), c19orf10-FLAG (40 ng/ml) + anti-c19orf10 antibodies (gray bar) and c19orf10-FLAG (40 ng/ml) + control mouse IgG (black bar).

HuH7 cells. We observed an ~50% decrease in *c19orf10* expression in Hep3B cells transfected with Si- *c19orf10* compared to the control 48 hr after transfection with statistical significance ($p < 0.0001$). In this condition, cell proliferation was suppressed to 50% compared to the control 72 hr after transfection ($p < 0.0001$) (Figs. 3*c* and 3*d*). When we performed cell cycle analysis of HuH7 cells transfected with Si-*Control* or Si-*c19orf10*, we identified an increase of G1-phase cells and a decrease of S- and G2-phase cells by *c19orf10* knockdown, suggesting that the G1 cycle arrest was caused by the knockdown of *c19orf10* (Fig. 3*e*).

We examined the representative MAPK/Akt pathway-associated proteins and cell cycle regulators using Western blotting 72 hr after siRNAs transfection (Fig. 3*f*). Interestingly, phosphorylation of c-Raf, MEK, MAPK, PI3K and pAkt was inhibited by knockdown of *c19orf10*, suggesting the involvement of *c19orf10* in the MAPK/Akt pathways. Furthermore, phosphorylation of Rb, CDK4 and CDK6 was also inhibited by knockdown of *c19orf10*, consistent with the observation of G1 cell cycle arrest by *C19ORF10* knockdown. PTEN, p53 and phosphorylated CDC2 protein expression was not affected by knockdown of *c19orf10*.

C19orf10 encodes the secretory protein and stimulates cell proliferation

As the sequence of *c19orf10* suggested that it encodes a secretory protein, we transfected pSI-*c19orf10-FLAG* in NIH3T3 cells and examined the culture supernatant. Immunoprecipitation of the collected culture supernatant 48 hr after transfection using anti-FLAG antibodies indicated the existence of a 17-kDa protein (c19orf10), compatible with the molecular weight of the 142 amino acids protein encoded by *c19orf10* (Fig. 4*a*). We purified c19orf10-FLAG protein from the supernatant of HEK293 cells infected with Ad. *c19orf10-FLAG* using an anti-FLAG column. Supplementation of purified c19orf10-FLAG into the culture media for 72 hr enhanced the proliferation of HLE cells in a dose-dependent manner with statistical significance, whereas control FLAG peptides

and BSA had no effects on cell proliferation (Fig. 4*b*). Western blot analysis of HLE cells cultured with purified c19orf10-FLAG (40 ng/ml) or BSA control (40 ng/ml) indicated the immediate strong phospholyration of Akt peaked 5 min after supplementation (Fig. 4*c*). The modest phospholyration of GSK3β (Ser9) and p44/42 MAPK also followed and peaked 60 min after c19orf10 supplementation. These data suggest that Akt pathway might be directly involved in the c19orf10-mediated cell proliferation signaling with the subsequent activation of MAPK pathway. Furthermore, addition of antibodies against c19orf10 to the culture media abolished the cell proliferation induced by c19orf10, whereas control IgG had no effects (Fig. 4*d*). Taken together, these data suggest that c19orf10 may be a growth factor overexpressed in AFP-positive HCCs and activates the Akt/MAPK pathways, potentially through the activation of an unidentified c19orf10 receptor.

Discussion

SAGE facilitates the measurement of transcripts from normal and malignant tissues in a nonbiased and highly accurate, quantitative manner. Indeed, SAGE produces a comprehensive gene expression profile without *a priori* gene sequence information, leading to the identification of novel transcripts potentially involved in the pathogenesis of human cancer.[19] In our study, we identified seven SAGE tags potentially corresponding to novel genes activated in HCC. Among them, we identified the secretory protein c19orf10 activated in a subset of HCCs.

Several serum markers including AFP, DCP and Glypican 3 are currently used for the detection and/or the evaluation of the treatment for HCCs in the clinic.[15–18,35] These markers are known as oncofetal proteins, that is, expressed in the fetus, transcriptionally suppressed in the adult organ and reactivated in the tumor. We identified that the expression of *c19orf10* positively correlated with *AFP* expression but did not correlate with the expression of *GPC3* or the biliary marker *KRT19*. As *c19orf10* was rarely detected in the normal liver, it is possible that c19orf10 is also an oncofetal protein activated in HCC. We are currently developing a system to detect serum c19orf10 in HCC patients, and the significance of the serum c19orf10 value as an HCC marker should be clarified.

Recent advancement in molecular biology has revealed the considerable diversity of transcription initiation and/or termination of genes altered in the process of carcinogenesis. Indeed, using 5′ SAGE approach, we recently discovered the novel intronic transcripts activated in HCC.[36] Interestingly, when we investigated the transcription initiation of *c19orf10* using the 5′ SAGE database, we identified a potential 5′ splice variant initiated from the second exon of *c19orf10* (data not shown). Although we have not yet validated the presence of 5′ splice variants in *c19orf10* by PCR, examination of 5′ EST database also suggested the presence of the similar splice variants (GenBank Accession Number CR980295, BQ680744, BQ648461, *etc.*). Alteration of transcription initiation/termination in *c19orf10* might affect the abundance or function of c19orf10 protein, and the details of 5′ splice variants in *c19orf10* should be clarified in future studies.

Molecular targeting therapy has rapidly emerged for solid tumors as well as for leukemia.[37–39] Sorafenib is a multikinase inhibitor targeting Raf kinase in the MAPK pathway as well as VEGFR and the platelet-derived growth factor receptor.[40,41] In our study, we identified that c19orf10 activates the MAPK and Akt/PI3K pathways and contributes to the proliferation of HCC cell lines, although we still could not discover the potential receptor of c19orf10. Development of a neutralizing c19orf10 antibody may provide novel therapeutic options for HCC patients to inhibit these signaling pathways, and its efficacy should be evaluated in the future.

Recently, c19orf10 was found to be expressed in fibroblast-like synoviocytes in the synovium using a proteomics approach.[29] In addition, a recent article indicated that c19orf10 was expressed in preadipocyte cells and involved in adipogenesis using two-dimensional electrophoresis mass spectrometry analysis.[28] Thus, c19orf10 may have pleiotropic effects on various lineages of normal organs in various developmental stages, and the clarification of its distribution and biological properties in the whole body may provide more detailed information about the function of c19orf10.

In conclusion, we have identified the protein c19orf10 that regulates the Akt/MAPK pathways and cell cycle through an unidentified mechanism in HCC. Although further studies should be conducted to detect the potential c19orf10 receptor or signaling molecules binding to c19orf10, our study suggests that c19orf10 may be a novel growth factor, a potential tumor marker and also a potential target molecule for HCC treatment.

Acknowledgements

The authors thank Ms. Mikie Kakiuchi, Ms. Masayo Baba and Ms. Nami Nishiyama for their excellent technical assistance.

References

1. Befeler AS, Di Bisceglie AM. Hepatocellular carcinoma: diagnosis and treatment. *Gastroenterology* 2002;122:1609–19.
2. Tsukuma H, Hiyama T, Tanaka S, Nakao M, Yabuuchi T, Kitamura T, Nakanishi K, Fujimoto I, Inoue A, Yamazaki H, Kawashima T. Risk factors for hepatocellular carcinoma among patients with chronic liver disease. *N Engl J Med* 1993;328:1797–801.
3. Liang TJ, Jeffers LJ, Reddy KR, De Medina M, Parker IT, Cheinquer H, Idrovo V, Rabassa A, Schiff ER. Viral pathogenesis of hepatocellular carcinoma in the United States. *Hepatology* 1993;18:1326–33.
4. Mayans MV, Calvet X, Bruix J, Bruguera M, Costa J, Esteve J, Bosch FX, Bru C, Rodes J. Risk factors for hepatocellular carcinoma in Catalonia, Spain. *Int J Cancer* 1990;46:378–81.

5. Mohamed AE, Kew MC, Groeneveld HT. Alcohol consumption as a risk factor for hepatocellular carcinoma in urban southern African blacks. *Int J Cancer* 1992; 51:537–41.
6. Smedile A, Bugianesi E. Steatosis and hepatocellular carcinoma risk. *Eur Rev Med Pharmacol Sci* 2005;9:291–3.
7. Floreani A, Baragiotta A, Baldo V, Menegon T, Farinati F, Naccarato R. Hepatic and extrahepatic malignancies in primary biliary cirrhosis. *Hepatology* 1999; 29:1425–8.
8. Tradati F, Colombo M, Mannucci PM, Rumi MG, De Fazio C, Gamba G, Ciavarella N, Rocino A, Morfini M, Scaraggi A, Taioli E. A prospective multicenter study of hepatocellular carcinoma in italian hemophiliacs with chronic hepatitis C. The Study Group of the Association of Italian Hemophilia Centers. *Blood* 1998;91:1173–7.
9. Jones DE, Metcalf JV, Collier JD, Bassendine MF, James OF. Hepatocellular carcinoma in primary biliary cirrhosis and its impact on outcomes. *Hepatology* 1997; 26:1138–42.
10. Caballeria L, Pares A, Castells A, Gines A, Bru C, Rodes J. Hepatocellular carcinoma in primary biliary cirrhosis: similar incidence to that in hepatitis C virus-related cirrhosis. *Am J Gastroenterol* 2001; 96:1160–3.
11. Yoshida H, Shiratori Y, Moriyama M, Arakawa Y, Ide T, Sata M, Inoue O, Yano M, Tanaka M, Fujiyama S, Nishiguchi S, Kuroki T, et al. Interferon therapy reduces the risk for hepatocellular carcinoma: national surveillance program of cirrhotic and noncirrhotic patients with chronic hepatitis C in Japan. IHIT Study Group. Inhibition of Hepatocarcinogenesis by Interferon Therapy. *Ann Intern Med* 1999; 131:174–81.
12. Yuen MF, Cheng CC, Lauder IJ, Lam SK, Ooi CG, Lai CL. Early detection of hepatocellular carcinoma increases the chance of treatment: Hong Kong experience. *Hepatology* 2000;31:330–5.
13. Peterson MS, Baron RL. Radiologic diagnosis of hepatocellular carcinoma. *Clin Liver Dis* 2001;5:123–44.
14. Choi BI. The current status of imaging diagnosis of hepatocellular carcinoma. *Liver Transpl* 2004;10:S20–S25.
15. Fujiyama S, Tanaka M, Maeda S, Ashihara H, Hirata R, Tomita K. Tumor markers in early diagnosis, follow-up and management of patients with hepatocellular carcinoma. *Oncology* 2002;62 (Suppl 1):57–63.
16. Tsai SL, Huang GT, Yang PM, Sheu JC, Sung JL, Chen DS. Plasma des-gamma-carboxyprothrombin in the early stage of hepatocellular carcinoma. *Hepatology* 1990; 11:481–8.
17. Ikoma J, Kaito M, Ishihara T, Nakagawa N, Kamei A, Fujita N, Iwasa M, Tamaki S, Watanabe S, Adachi Y. Early diagnosis of hepatocellular carcinoma using a sensitive assay for serum des-gamma-carboxy prothrombin: a prospective study. *Hepatogastroenterology* 2002; 49:235–8.
18. Kasahara A, Hayashi N, Fusamoto H, Kawada Y, Imai Y, Yamamoto H, Hayashi E, Ogihara T, Kamada T. Clinical evaluation of plasma des-gamma-carboxy prothrombin as a marker protein of hepatocellular carcinoma in patients with tumors of various sizes. *Dig Dis Sci* 1993; 38:2170–6.
19. Yamashita T, Honda M, Kaneko S. Application of serial analysis of gene expression in cancer research. *Curr Pharm Biotechnol* 2008;9:375–82.
20. Cheng AL, Kang YK, Chen Z, Tsao CJ, Qin S, Kim JS, Luo R, Feng J, Ye S, Yang TS, Xu J, Sun Y, et al. Efficacy and safety of sorafenib in patients in the Asia-Pacific region with advanced hepatocellular carcinoma: a phase III randomised, double-blind, placebo-controlled trial. *Lancet Oncol* 2009;10:25–34.
21. Llovet JM, Ricci S, Mazzaferro V, Hilgard P, Gane E, Blanc JF, de Oliveira AC, Santoro A, Raoul JL, Forner A, Schwartz M, Porta C, et al. Sorafenib in advanced hepatocellular carcinoma. *N Engl J Med* 2008;359:378–90.
22. Yamashita T, Hashimoto S, Kaneko S, Nagai S, Toyoda N, Suzuki T, Kobayashi K, Matsushima K. Comprehensive gene expression profile of a normal human liver. *Biochem Biophys Res Commun* 2000;269: 110–16.
23. Yamashita T, Honda M, Takatori H, Nishino R, Hoshino N, Kaneko S. Genome-wide transcriptome mapping analysis identifies organ-specific gene expression patterns along human chromosomes. *Genomics* 2004;84:867–75.
24. Yamashita T, Honda M, Takatori H, Nishino R, Minato H, Takamura H, Ohta T, Kaneko S. Activation of lipogenic pathway correlates with cell proliferation and poor prognosis in hepatocellular carcinoma. *J Hepatol* 2009;50:100–10.
25. Yamashita T, Kaneko S, Hashimoto S, Sato T, Nagai S, Toyoda N, Suzuki T, Kobayashi K, Matsushima K. Serial analysis of gene expression in chronic hepatitis C and hepatocellular carcinoma. *Biochem Biophys Res Commun* 2001;282:647–54.
26. Tulin EE, Onoda N, Nakata Y, Maeda M, Hasegawa M, Nomura H, Kitamura T. SF20/IL-25, a novel bone marrow stroma-derived growth factor that binds to mouse thymic shared antigen-1 and supports lymphoid cell proliferation. *J Immunol* 2001;167:6338–47.
27. Tulin EE, Onoda N, Nakata Y, Maeda M, Hasegawa M, Nomura H, Kitamura T. SF20/IL-25, a novel bone marrow stroma-derived growth factor that binds to mouse thymic shared antigen-1 and supports lymphoid cell proliferation. *J Immunol* 2003;170:1593.
28. Wang P, Mariman E, Keijer J, Bouwman F, Noben JP, Robben J, Renes J. Profiling of the secreted proteins during 3T3-L1 adipocyte differentiation leads to the identification of novel adipokines. *Cell Mol Life Sci* 2004;61:2405–17.
29. Weiler T, Du Q, Krokhin O, Ens W, Standing K, El-Gabalawy H, Wilkins JA. The identification and characterization of a novel protein, c19orf10, in the synovium. *Arthritis Res Ther* 2007;9:R30.
30. Takatori H, Yamashita T, Honda M, Nishino R, Arai K, Takamura H, Ohta T, Zen Y, Kaneko S. dUTP pyrophosphatase expression correlates with a poor prognosis in hepatocellular carcinoma. *Liver Int* 2010; 30:438–46.
31. Sakai Y, Honda M, Fujinaga H, Tatsumi I, Mizukoshi E, Nakamoto Y, Kaneko S. Common transcriptional signature of tumor-infiltrating mononuclear inflammatory cells and peripheral blood mononuclear cells in hepatocellular carcinoma patients. *Cancer Res* 2008;68: 10267–79.
32. Honda M, Yamashita T, Ueda T, Takatori H, Nishino R, Kaneko S. Different signaling pathways in the livers of patients with chronic hepatitis B or chronic hepatitis C. *Hepatology* 2006;44:1122–38.
33. Sakai Y, Morrison BJ, Burke JD, Park JM, Terabe M, Janik JE, Forni G, Berzofsky JA, Morris JC. Vaccination by genetically modified dendritic cells expressing a truncated neu oncogene prevents development of breast cancer in transgenic mice. *Cancer Res* 2004;64:8022–8.
34. Sakai Y, Kaneko S, Nakamoto Y, Kagaya T, Mukaida N, Kobayashi K. Enhanced anti-tumor effects of herpes simplex virus thymidine kinase/ganciclovir system by codelivering monocyte chemoattractant protein-1 in hepatocellular carcinoma. *Cancer Gene Ther* 2001;8:695–704.
35. Capurro M, Wanless IR, Sherman M, Deboer G, Shi W, Miyoshi E, Filmus J. Glypican-3: a novel serum and histochemical marker for hepatocellular carcinoma. *Gastroenterology* 2003;125: 89–97.
36. Hodo Y, Hashimoto S, Honda M, Yamashita T, Suzuki Y, Sugano S, Kaneko S, Matsushima K. Comprehensive gene expression analysis of 5′-end of mRNA identified novel intronic transcripts associated with hepatocellular carcinoma. *Genomics* 2010;95:217–23.

37. Romond EH, Perez EA, Bryant J, Suman VJ, Geyer CE, Jr, Davidson NE, Tan-Chiu E, Martino S, Paik S, Kaufman PA, Swain SM, Pisansky TM, et al. Trastuzumab plus adjuvant chemotherapy for operable HER2-positive breast cancer. *N Engl J Med* 2005;353:1673–84.
38. Hurwitz H, Fehrenbacher L, Novotny W, Cartwright T, Hainsworth J, Heim W, Berlin J, Baron A, Griffing S, Holmgren E, Ferrara N, Fyfe G, et al. Bevacizumab plus irinotecan, fluorouracil, and leucovorin for metastatic colorectal cancer. *N Engl J Med* 2004;350:2335–42.
39. Shepherd FA, Rodrigues Pereira J, Ciuleanu T, Tan EH, Hirsh V, Thongprasert S, Campos D, Maoleekoonpiroj S, Smylie M, Martins R, van Kooten M, Dediu M, et al. Erlotinib in previously treated non-small-cell lung cancer. *N Engl J Med* 2005; 353:123–32.
40. Llovet JM, Bruix J. Molecular targeted therapies in hepatocellular carcinoma. *Hepatology* 2008;48:1312–27.
41. Liu L, Cao Y, Chen C, Zhang X, McNabola A, Wilkie D, Wilhelm S, Lynch M, Carter C. Sorafenib blocks the RAF/MEK/ERK pathway, inhibits tumor angiogenesis, and induces tumor cell apoptosis in hepatocellular carcinoma model PLC/PRF/5. *Cancer Res* 2006;66: 11851–8.

Cancer Letters 307 (2011) 165–173

Contents lists available at ScienceDirect

Cancer Letters

journal homepage: www.elsevier.com/locate/canlet

Frequency of CD45RO$^+$ subset in CD4$^+$CD25^{high} regulatory T cells associated with progression of hepatocellular carcinoma

Yoshiko Takata [a], Yasunari Nakamoto [a], Akiko Nakada [b], Takeshi Terashima [a], Fumitaka Arihara [a], Masaaki Kitahara [a], Kaheita Kakinoki [a], Kuniaki Arai [a], Taro Yamashita [a], Yoshio Sakai [a], Tatsuya Yamashita [a], Eishiro Mizukoshi [a], Shuichi Kaneko [a,*]

[a] *Disease Control and Homeostasis, Graduate School of Medicine, Kanazawa University, 13-1 Takara-machi, Kanazawa 920-8641, Japan*
[b] *Otsuka Pharmaceutical Co., Ltd., 2-16-4 Konan, Minato-ku, Tokyo 108-8242, Japan*

ARTICLE INFO

Article history:
Received 31 December 2010
Received in revised form 11 March 2011
Accepted 30 March 2011

Keywords:
Regulatory T cell
Dendritic cell
Hepatocellular carcinoma
CD45RO
Intracellular cytokine

ABSTRACT

The purpose of this study was to assess the properties of CD4$^+$CD25$^{high/low/negative}$ T cell subsets and analyze their relation with dendritic cells (DCs) in patients with hepatocellular carcinoma (HCC). In HCC patients, the prevalence of CD45RO$^+$ cells in CD4$^+$CD25^{high} T cells was increased and associated with higher frequencies of plasmacytoid DCs. Larger proportions of this T cell subset were detected in the patients with larger tumor burdens. These results suggest that increased frequencies of the CD45RO$^+$ subset in CD4$^+$CD25^{high} Tregs in HCC patients may establish the immunosuppressive environment cooperatively with tolerogenic plasmacytoid DCs to promote disease progression of liver cancer.

1. Introduction

Hepatocellular carcinoma (HCC) occurs primarily in individuals with cirrhosis related to hepatitis C virus (HCV) or hepatitis B virus (HBV) infections, and alcohol abuse. HCC is the fifth most common cancer, with increasing incidence worldwide. It is characterized by high mortality, frequent postsurgical recurrence and extremely poor prognosis [1–3].

CD4$^+$CD25^{high} Foxp3$^+$ regulatory T cells (Tregs) have been shown to suppress immune responses by direct interaction with other immune cell types or through immune suppressive cytokines and appear crucial in maintaining immune homeostasis, mediating peripheral tolerance and preventing autoimmunity [4–6]. Increased frequencies of Tregs have been documented in the peripheral blood and in some cases the tumor microenvironment in patients with several different tumor types [3–12]. It has been reported that, in HCC patients, increased Tregs are correlated with CD8$^+$ T-cell impairment [11] and are related to poor prognosis [1].

Tregs are known to consist of heterogeneous subsets and to express various surface markers detectable by flow cytometry, including CD45RO, CTLA-4 (cytotoxic T lymphocyte associated antigen-4), GITR (glucocorticoid-induced TNF receptor-related protein), CD62L, HLA-DR, and CCR7 [8,13–15]. The role of these markers in suppressor functions mediated by human Tregs is currently under discussion [8]. It has been suggested that GITR is associated with T cell activation [16,17] and Treg subset expressing GITR are associated with disease activity in patients with Wegener's granulomatosis [17]. As for HCC, Ormandy et al. demonstrated that Tregs in HCC patients expressed high levels of HLA-DR and GITR [3]. However, there is a paucity of studies presenting the association of Treg subsets with disease progression.

In addition to Tregs, dendritic cells (DCs), a type of professional antigen-presenting cells (APCs), may be

* Corresponding author. Tel.: +81 76 265 2233; fax: +81 76 234 4250.
E-mail address: skaneko@m-kanazawa.jp (S. Kaneko).

0304-3835/$ - see front matter © 2011 Published by Elsevier Ireland Ltd.
doi:10.1016/j.canlet.2011.03.029

implicated in the regulation of immune responses. The role of human DCs in modulating Tregs is not clear [18]. It has been suggested that immature and mature myeloid DCs (mDCs) and plasmacytoid DCs (pDCs) may promote Treg cell differentiation, homeostasis and function [19]. It has been shown that lung cancer cells can convert mature DCs into TGF-β1 producing cells, which demonstrate an increased ability to generate Tregs [20]. Conversely, Tregs can induce the generation of semimature DCs by which they can down-regulate immune responses [21]. These data suggest that there may be a mutual interaction between Tregs and DCs for the maintenance of immunosuppression.

In the present study, we evaluated the frequency and properties of $CD4^+CD25^{high}$ $Foxp3^+$ T cells in HCC patients. Increased numbers of these cells produced more Th2 cytokine than $CD4^+CD25^{low/negative}$ cells. Furthermore, the proportion of $CD45RO^+$ subset was increased in HCC patients. We also analyzed how the subset is related to DC frequencies, and found that some subsets were relevant to disease progression.

2. Materials and methods

2.1. Patients and healthy controls

Sixty-two HCC patients attending Kanazawa University Hospital (Ishikawa, Japan) between September 2006 and July 2008 were enrolled in this study with their informed consent. HCC was radiologically diagnosed by computed tomography (CT), magnetic resonance imaging (MRI), and CT angiography. Blood samples were taken from these HCC patients, as well as from 41 healthy controls, 17 patients with chronic hepatitis (CH) B and C and 16 patients with liver cirrhosis (LC) without a tumor. None of the patients received anticancer nor antiviral therapy at time of blood sample. Patients characteristics and disease classification are shown in Table 1.

Table 1
Clinical characteristics of hepatocellular carcinoma, liver cirrhosis, chronic hepatitis patients and healthy control.

Hepatocellular carcinoma (n = 62)	
Age (yrs)	68.9 ± 9.5
Gender (M/F)	37/25
Etiology of liver disease	
HBV/HCV/HBV + HCV/NBNC	19/34/2/7
TNM stages I/II/III/IV-A/IV-B	18/12/20/6/6
Largest tumor (mm)	
Child-Pugh A/B/C	37.6 ± 34.4
AFP (ng/mL)	41/8/3
DCP (mAU/mL)	10–35,093 (52)
Liver cirrhosis (n = 16)	
Age (yrs)	10–32,818 (34)
Gender (M/F)	58.3 ± 10.3
Etiology of liver disease	11/5
HBV/HCV/NBNC	4/7/5
Chronic hepatitis (n = 17)	
Age (yrs)	58.9 ± 10.4
Gender (M/F)	8/9
Etiology of liver disease	
HBV/HCV/NBNC	0/17/0
Healthy controls (n = 41)	
Age (yrs)	46.1 ± 19.1
Gender (M/F)	16/25

Note: Results except for AFP and DCP are expressed as means ± SD. AFP and DCP values are expressed as range (median). The reference range of normal values for the laboratory values: AFP < 10 ng/mL, DCP < 40 mAU/mL. M, Male; F, Female; HBV, hepatitis B virus; HCV, hepatitis C virus; NBNC, non-B non-C; TNM, tumor-node-metastasis; AFP, alpha-fetoprotein; DCP, des-gamma-carboxy prothrombin.

2.2. Isolation of PBMC and $CD4^+$ T cells

Peripheral blood mononuclear cells (PBMC) were isolated from freshly obtained blood by Ficoll-Hypaque (Sigma–Aldrich, St. Louis, MO). Total cell numbers were counted in the presence of a trypan blue dye to evaluate viability and immediately used for experiments. $CD4^+$ T cells were isolated from fleshly isolated PBMC by negative magnetic selection using the $CD4^+$ T Cell Isolation Kit II (Miltenyi Biotec, Bergisch Gladbach, Germany) and QuadroMACS Separation Unit (Miltenyi Biotec) according to the manufacturer's instruction. Isolated $CD4^+$ T cells were purified by >90% as measured by flow cytometric analysis using a FACSCaliber flow cytometer (BD Biosciences, San Jose, CA).

2.3. Antibodies

The following anti-human monoclonal antibodies (mAb) were used for flow cytometry: anti-CD4-PerCP, anti-CD25-APC (BD Biosciences, San Jose, CA), anti-CD45RO-FITC (PROIMMUNE, Oxford, UK), anti-CTLA-4-PE, anti-CCR7-PE, anti-GITR (glucocorticoid-induced TNF receptor-related protein)-PE (R&D Systems, Minneapolis, MN), anti-CD62L-FITC, anti-HLA-DR-FITC, anti-CD45RA-PE (Exalpha Biologicals, Watertown, MA), IOTest Conjugated Antibodies – (CD14 + CD16)-FITC/CD85k(ILT3)-PE/CD123-PC5 Dendritic Cells " Plasmacytoid Subset " and IOTest Conjugated Antibodies – (CD14 + CD16)-FITC/CD85k(ILT3)-PE/CD33-PC5 Dendritic Cells "Myeloid Subset " (Beckman Coulter, Miami, FL). Before use, all mAbs were titrated using normal PBMC to establish optimal staining dilutions.

2.4. Surface and intracellular staining

To determine the frequency of $CD4^+CD25^{high}$ T cells and the surface marker profile, $CD4^+$ T cells (at least 2×10^5 cells/tube) were stained with mAbs in the above described panel for 30 min on ice. Apropriate isotype antibody controls were used for each sample. Cells were washed and examined by four-color flow cytometry.

For intracellular Foxp3 and cytokine staining, 2×10^5 $CD4^+$ T cells/well in a 96-plate were stimulated with Leucocyte Activation Cocktail containing PMA, ionomycin, and brefeldin A, and then cultured at 37 °C in a humidified CO_2 incubator for 4 h. The activated cells were first incubated with anti-CD4-PerCP for 15 min on ice, followed by fixation and permeabilization of the activated cells for 20 min at room temperature with BD Cytofix/Cytoperm Buffer (BD Biosciences, San Diego, CA). Samples were then stained with anti-CD25-APC, anti-Foxp3-FITC (eBioscience) and PE-labeled anti-cytokine (IL-4, IL-10) antibodies (BD

Biosciences) for 15 min at room temperature. Apropriate isotype controls were included for each sample.

2.5. Flow cytometric analysis

The samples were acquired on a FACSCalibur for four-color flow cytometry. Data analysis was performed using the CellQuest software (Becton Dickinson, CA, USA).

2.6. Statistical analysis

Data are indicated as means ± SD unless otherwise stated. The statistical significance of difference between the two groups was determined by applying the Mann–Whitney nonparametric U test. $P < 0.05$ was considered significant.

3. Results

3.1. Frequencies of $CD4^+CD25^{high}$ T cells

To evaluate the frequencies of $CD4^+CD25^{high}$ T cell subsets that contain Tregs, MACS-sorted $CD4^+$ T cell subsets obtained from the patients with CH, LC and HCC and healthy controls were analyzed by flow cytometry following the staining with anti-CD4 and anti-CD25 monoclonal antibodies (Fig. 1A and B). Although the frequencies of $CD4^+CD25^{high}$ T cells were not changed in patients with CH, they were increased in patients with LC compared to the controls ($P < 0.05$). As reported, it is remarkably elevated in patients with HCC ($P < 0.0001$). The results indicated that $CD4^+CD25^{high}$ T cell subset containing Tregs are increased in patients complicated with liver malignancies.

3.2. Intracellular Foxp3 and cytokine production of the $CD4^+CD25^{high}$ T cell subset in HCC patients

The transcription factor Foxp3 is considered to be a specific marker for Tregs [22–24]. Intracellular Foxp3 levels were detected by using the specific mAb after the cell membrane permeabilization procedures (Fig. 2A). The percent of $Foxp3^+$ cells in the $CD4^+CD25^{high}$ T cell subset in HCC patients was larger than that of $CD4^+CD25^{low/negative}$ subset, and it was also significantly larger than that of $CD4^+CD25^{high}$ T cells in healthy controls and CH patients (Fig. 2B). Thus, not only is the number of $CD4^+CD25^{high}$ T cells in HCC patients larger, but also the frequency of $Foxp3^+$ cells in HCC patients is higher than CH patient and healthy controls. This is consistent with previous reports of Tregs in patients with other malignancies.

Intracellular production of cytokines IL-4 and IL-10 of $CD4^+CD25^{high}$-$Foxp3^+$ T cell subset was quantitated following the stimulation with PMA/ionomycin using the specific mAbs by flow cytometry (Fig. 2C).

The levels of Th2 cytokines IL-4 and IL-10 were high in the $CD4^+CD25^{high}$ subsets. In addition, the levels of IL-4 and IL-10 were high in the $CD4^+CD25^{high}Foxp3^+$ T cell subset in HCC patient ($P < 0.005$) (Fig. 2D). These results suggest that the $CD4^+CD25^{high}Foxp3^+$ Treg subset in HCC patients may have a high potential to produce immunosuppressive cytokines.

3.3. Phenotypes of the $CD4^+CD25^{high}$ T cell subset in HCC patients

To determine the phenotypical properties of $CD4^+CD25^{high}$ T cell subset increased in patients with HCC, the expression levels of the seven reported surface molecules, CD45RA, CD45RO, CD62L, CCR7, CTLA-4, HLA-DR and GITR were quantitated by flow cytometry. Among the seven molecules, the proportions of $CD45RO^+$, $HLA\text{-}DR^+$ and $GITR^+$ cells were higher in the $CD4^+CD25^{high}$ T cell subset in all patient groups compared to the $CD4^+CD25^{low/negative}$ T cell subsets, except for $GITR^+$ cells in CH patients ($P < 0.05$) (Fig. 3A and B). The percentage of $CD45RO^+$ cells in HCC patients were elevated compared to the patients with advanced liver diseases and healthy controls ($P < 0.01$). These data demonstrate that the $CD4^+CD25^{high}$ T cell subset highly expresses the surface molecule CD45RO in HCC patients, which may reflect the memory properties of T cells.

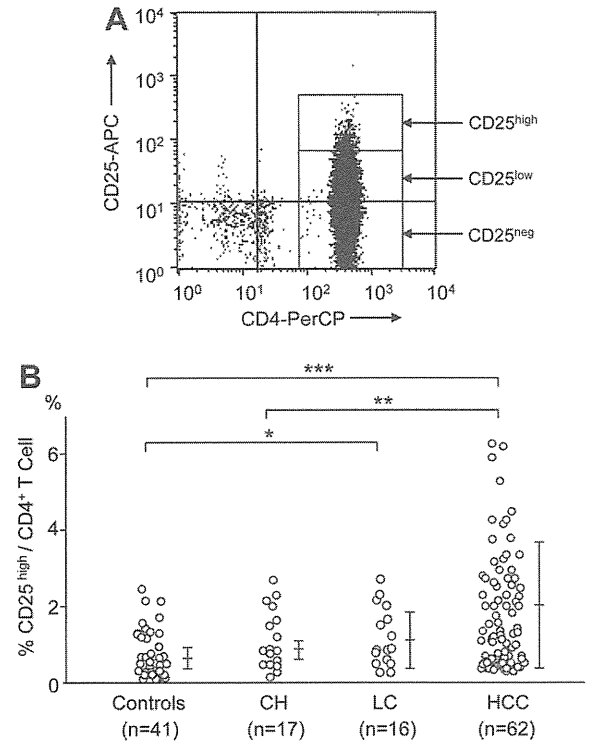

Fig. 1. Frequencies of $CD4^+CD25^{high}$ T cells in peripheral blood of HCC patients and controls. (A) Representative flow cytometric analysis of PBMCs (peripheral blood mononuclear cells) of an HCC patient. Freshly isolated PBMCs were labeled with anti-CD4 and anti-CD25 antibodies as described in the Materials and Methods. (B) Percentages of $CD4^+CD25^{high}$ T cells in the peripheral blood of HCC ($n = 62$), LC ($n = 16$), CH ($n = 17$) patient, and healthy controls ($n = 41$). Percentages for individual patient analyzed are shown. The percentages represent the proportions of $CD4^+CD25^{high}$ T cells in total $CD4^+$ cells. The prevalence of $CD4^+CD25^{high}$ T cells in HCC patients was significantly higher than in healthy controls or CH patients. CH, chronic hepatitis; HCC, hepatocellular carcinoma; LC, liver cirrhosis. *Indicates $P < 0.05$, **indicates $P < 0.01$ and ***indicates $P < 0.001$.

3.4. $CD4^+CD25^{high}$ T Cell subset and dendritic cells of HCC patients

Several reports have suggested that the $CD4^+CD25^{high}$ T cell subset may interact with dendritic cells. To evaluate the frequencies of DCs in PBMC of HCC patients, whole blood cells were analyzed by flow cytometry following the staining with IOTest Conjugated Antibodies – (CD14 + CD16)-FITC/CD85k(ILT3)-PE/CD123-PC5 Dendritic Cells "Plasmacytoid Subset" and IOTest Conjugated Antibodies – (CD14 + CD16)-FITC/CD85k(ILT3)-PE/CD33-PC5 Dendritic Cells "Myeloid Subset". HCC patients were divided into two groups according to the frequencies of $CD45RO^{positive}$ cells in $CD4^+CD25^{high}$ T cell subsets ($CD45RO^+$ vs. $CD45RO^{++}$). Patients with $CD45RO^{++}$ contained >83.8% positive cells in $CD4^+CD25^{high}$ T cells. The frequencies of $CD123^+$ plasmacytoid DCs were significantly higher in $CD45RO^{++}$, group ($P < 0.05$) (Fig. 5A and B), although those of $CD33^+$ myeloid DCs were not correlated with the subsets in $CD4^+CD25^{high}$ cells. These results showed that there are more tolerogenic plasmacytoid DCs in the PBMCs of HCC patients with higher frequencies of a memory subset of $CD4^+CD25^{high}$ T cells.

3.5. $CD4^+CD25^{high}$ T cell subset and tumor progression

To evaluate the association between $CD4^+CD25^{high}$ T cell phenotype and tumor progression, we compared the maximum tumor diameters, the number of tumors, tumor markers AFP (alpha-fetoprotein) and DCP (des-gamma-carboxyl prothrombin), TNM stages, Child-Pugh scores

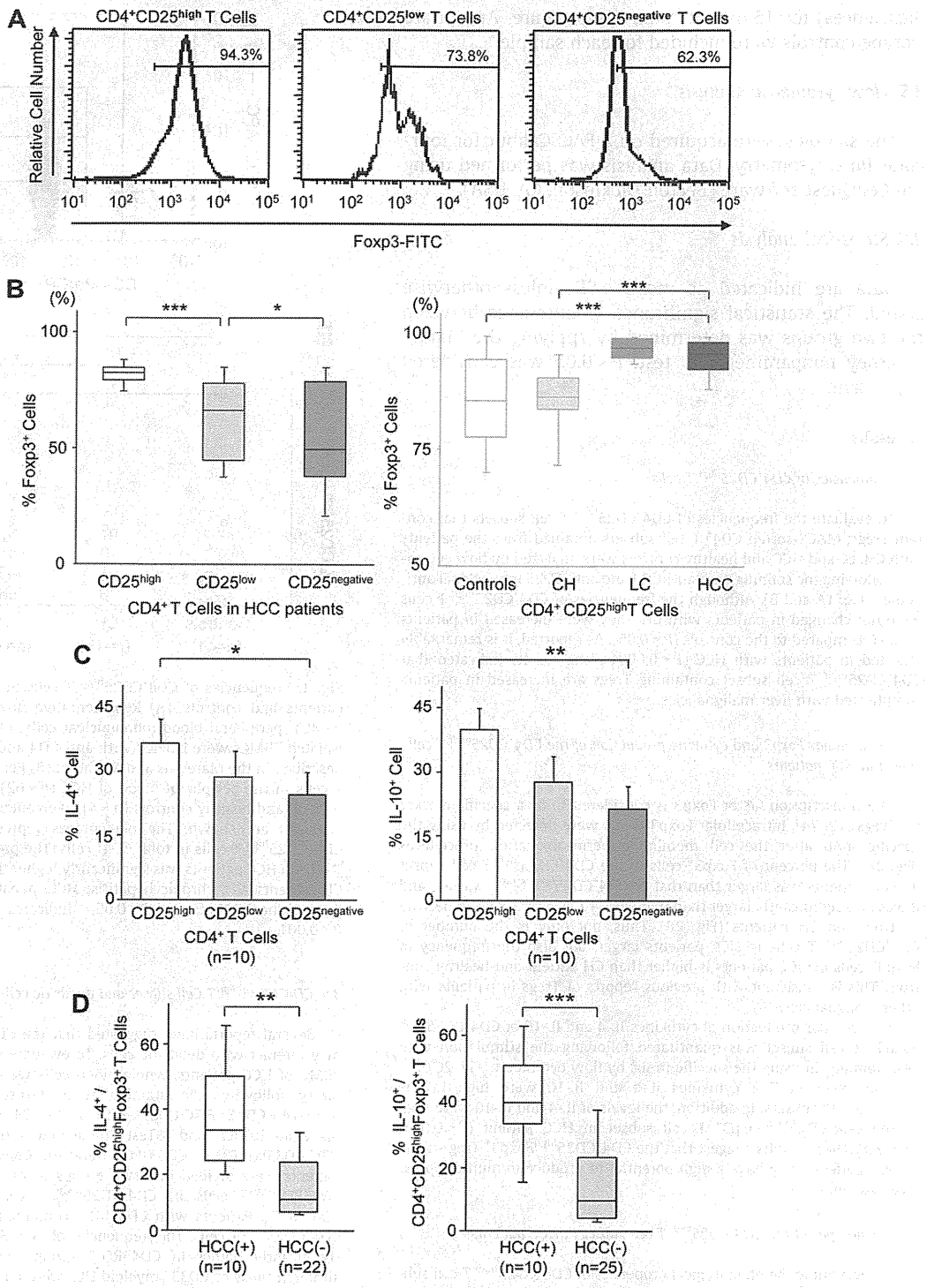

Fig. 2. Analysis of intracellular Foxp3 expression and cytokine production in $CD4^+$ $CD25^{high/low/negative}$ T cell subsets in HCC patients. (A) Representative expression of Foxp3 in $CD4^+$ T cells from an individual subject. Intracellular Foxp3 was stained following membrane permeabilization. Intracellular Foxp3 was detected by the specific mAb. (B) Statistical analysis in the left side panel shows that the percent of $Foxp3^+$ cells in the $CD4^+CD25^{high}$ T cell subset in HCC patients was significantly larger than that of $CD4^+CD25^{low/negative}$ T cell subsets, and in the right side panel shows that that of $CD4^+CD25^{high}$ T cell subset in HCC patients was significantly larger than that of $CD4^+CD25^{high}$ T cells in healthy controls and CH patients. (C) Statistical analysis shows that the levels of Th2 cytokines IL-4 and IL-10 were remarkably high in the $CD4^+CD25^{high}$ T cell subset. (D) Comparison of intracellular cytokine production in $CD4^+CD25^{high}$ T cell subsets between patients with and without HCC. Healthy controls, patients with chronic hepatitis and liver cirrhosis were included in the HCC (−) column. IL-4 and IL-10 levels were higher in the $CD4^+CD25^{high}$ T cell subset in HCC patients. *Indicates $P < 0.05$, **indicates $P < 0.01$ and ***indicates $P < 0.001$.

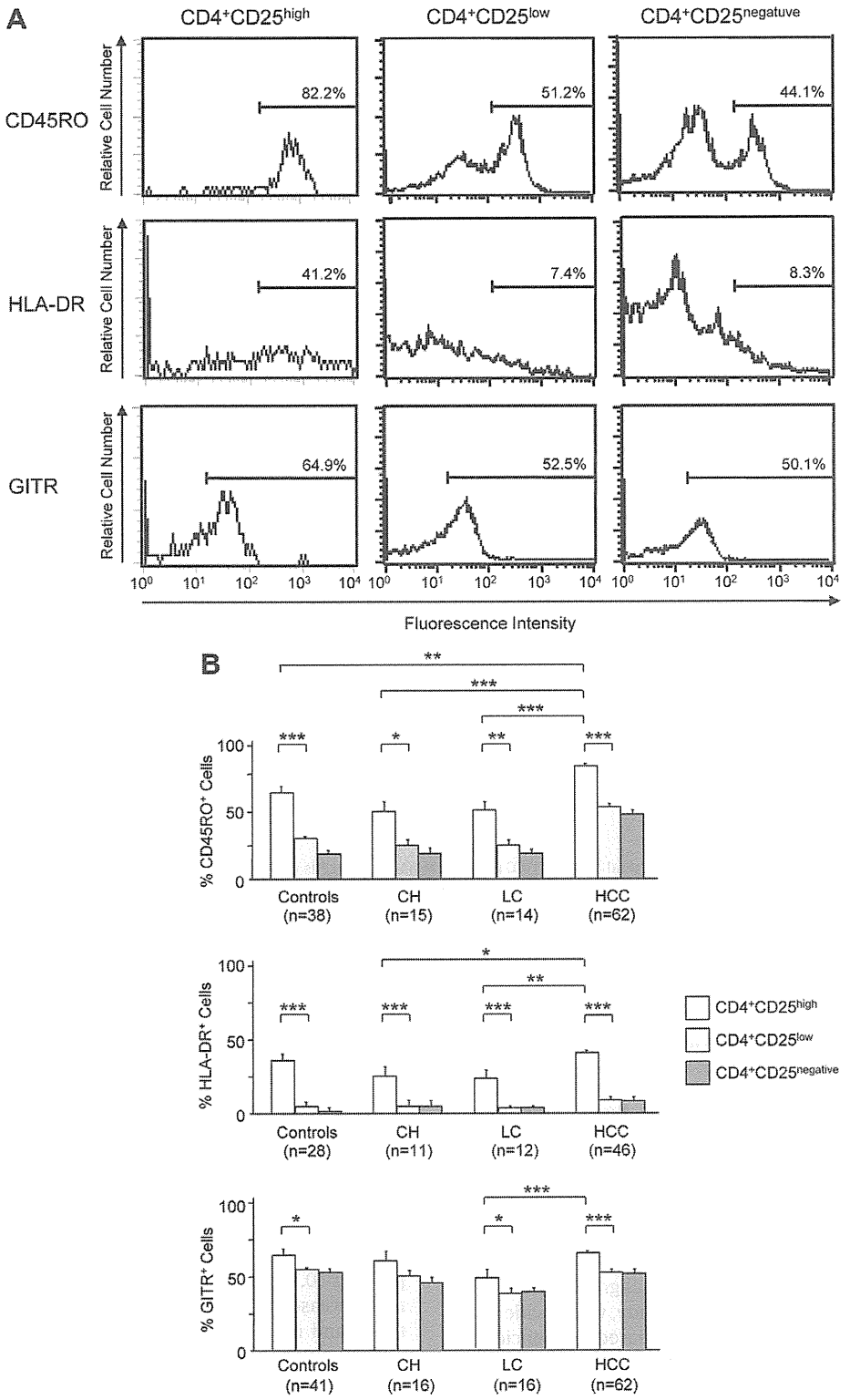

Fig. 3. Phenotypic analysis of $CD4^+CD25^{high/low/negative}$ T cell subsets in HCC patients. Fleshly isolated $CD4^+$ T cells (at least 2×10^5 cells/tube) from HCC patients were labeled with anti-CD4, anti-CD25, anti-CD45RA, anti-CD45RO, anti-CD62L, anti-CCR7, anti-CTLA-4, anti-HLA-DR and anti-GITR mAbs. (A) Representative CD45RO, HLA-DR, and GITR expression profiles in $CD4^+$ T cell subsets that differ in CD25 expression. (B) Statistical analysis shows that the proportions of $CD45RO^+$, $HLA\text{-}DR^+$ and $GITR^+$ were elevated in the $CD4^+CD25^{high}$ T cell subsets of all patient groups compared to the $CD4^+CD25^{low/negative}$ T cell subsets, except for $GITR^+$ cells in CH patients ($P < 0.05$). The percentage of $CD45RO^+$ cells in HCC patients was elevated compared to the patients with advanced liver diseases and healthy controls. *Indicates $P < 0.05$, **indicates $P < 0.01$ and ***indicates $P < 0.001$.

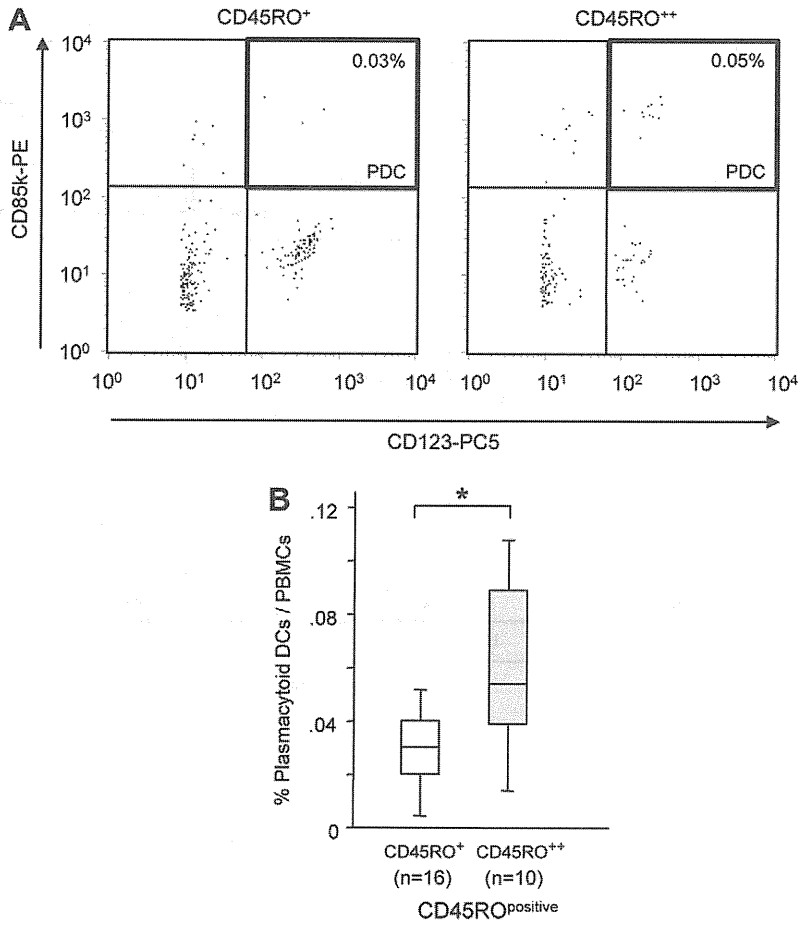

Fig. 4. Frequencies of plasmacytoid DCs in peripheral blood of HCC patients. Whole blood cells were analyzed by flow cytometry following staining with a combination of the mAbs. HCC patients were divided into two groups according to the frequencies of $CD45RO^{positivee}$ cells in $CD4^+CD25^{high}$ T cell subset ($CD45RO^+$ vs. $CD45RO^{++}$). Patients with $CD45RO^{++}$ contained > 83.8% positive cells in $CD4^+CD25^{high}$ T cells. (A) Representative dot plots of plasmacytoid DCs. Plasmacytoid DCs of $CD45RO^+$ group are shown in the left panel and $CD45RO^{++}$ group in the right panel. (B) Statistical analysis shows that the frequencies of plasmacytoid DCs were significantly higher in $CD45RO^{++}$ group. *Indicates $P < 0.05$.

and fibrosis stages between two groups as described above. The levels of serum AFP and DCP and the maximum tumor diameters in $CD45RO^{++}$ group were larger than those in $CD45RO^+$ group (Fig. 4). Others were not significantly different between two groups. These results imply that a subset of Tregs may contribute to the progression of liver tumors.

4. Discussion

$CD4^+CD25^{high}$ $Foxp3^+$ regulatory T cells have been shown to increase in patients with malignancies to suppress the immune responses. In this study, we provide evidence that patients with HCC have increased frequencies of $CD4^+CD25^{high}$ T cells in their peripheral blood compared to healthy controls and chronic hepatitis patients. A large proportion of $CD4^+CD25^{high}$ T cells expressed Foxp3 and produced Th2 cytokines. We also showed that $CD4^+CD25^{high}$ T cells expressed high levels of CD45RO, HLA-DR and GITR, and, interestingly, the T cell frequencies expressing these surface molecules were associated with plasmacytoid DC numbers and maximum tumor diameters in HCC patients.

There are several reports of elevated numbers of Treg cells in the peripheral blood and tumor tissues of patients with different types of cancer [3–12]. The study of Unitt et al. provided the first report of increased $CD4^+CD25^+$ T cell frequency within tumor tissue compared to non-tumor tissue in HCC patients [13]. Ormandy et al. showed that the frequency of $CD4^+CD25^{high}$ T cells in peripheral blood of patients with HCC was significantly higher ($3.92 \pm 3.3\%$) than in healthy donors ($1.17 \pm 0.87\%$) and liver cirrhosis patients ($0.78 \pm 0.43\%$) [3]. Our data revealed that a minimal increase in $CD4^+CD25^{high}$ T cells was detected in LC patients and more pronounced changes were found in HCC patients.

We showed that higher percentages of $CD4^+CD25^{high}$ T cells produced Th2 cytokines IL-4 and IL-10 in HCC patients. Tregs were recently observed to produce IL-10 [25–27], which can be a major mediator of immune suppression [28–30]. Voo et al. reported that Tregs in the peripheral blood of healthy donors secreted IL-10 but not IL-2, IFN-γ, or IL-4 [31]. Schmitz-Winnenthal et al. demon-

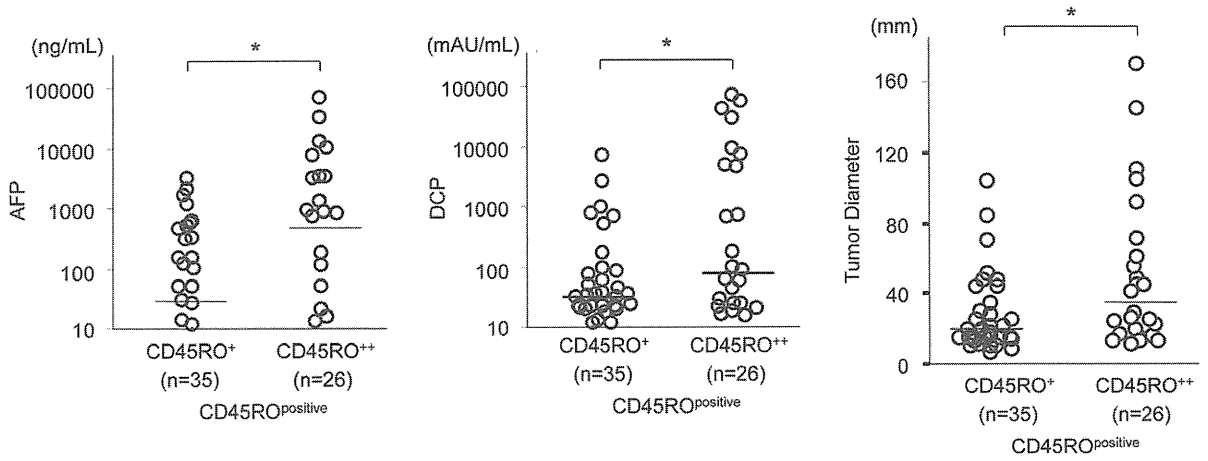

Fig. 5. Prevalence of $CD4^+CD25^{high/low/negative}$ T cell subsets and tumor progression. The levels of AFP and DCP and the maximum tumor diameters in $CD45RO^{++}$ group were larger than those in $CD45RO^+$ groups. AFP, alpha-fetoprotein; DCP, des-gamma-carboxyl prothrombin. *Indicates $P < 0.05$.

strated the presence of Treg secreting IL-10 but not IL-4 or IFN-γ upon antigen recognition in chronic pancreatitis patients [32]. The present data demonstrated that larger numbers of Tregs produced not only IL-10 but also IL-4 in HCC patients, which may contribute to the strong immunosuppressive properties of the T cells in liver malignancies.

It appears that Tregs consists of heterogenous populations within $CD4^+$ T cells, and that a subset of $CD4^+CD25^{high}$ T cells could be subdivided into different functional subsets based on the expression of various surface molecules [6]. The proportions of Tregs expressing these molecules are reported to be different in the various forms of cancer. The prevalence of $CD45RO^+$ and $GITR^+$ Treg cells is higher in $CD4^+CD25^{high}$ T cells than in $CD4^+CD25^{low/negative}$ T cells in renal cell carcinoma [4]. In head and neck squamous cell carcinoma, however, $CD4^+CD25^{high}$ T cells express CTLA-4, Foxp3, and CD62L but little GITR, and $CD25^{low/negative}$ T cells express intermediate to high levels of GITR and HLA-DR [8]. Our study showed that Tregs in HCC patients expressed significantly higher levels of CD45RO, HLA-DR and GITR compared to $CD4^+CD25^{low/negative}$ cells, suggesting that the activated populations of Tregs may contribute to the establishment of immunosuppressive microenvironments.

Little is known about the molecular and cellular mechanisms responsible for the increase and maintenance of elevated numbers of Treg cells in cancer. DCs have pivotal roles in the induction of tolerogenic/regulatory T cells [20,33]. In peripheral blood, there are two distinct populations of DCs which can be distinguished based on phenotypical and morphological characteristics; myeloid DCs (mDCs) and plasmacytoid DCs (pDCs) [18,34]. Our data demonstrated that higher frequencies of $CD45RO^+CD4^+CD25^{high}$ T cells were associated with higher frequencies of pDCs in the peripheral blood of HCC patients. When the tumor antigens are assumed by pDCs through Toll-like receptor 9 (TLR9) via receptor-mediated endocytosis, secretions of pro-inflammatory cytokines, such as type I interferons (IFNs), would be caused. On the contrary, pDC may regulate anti-tumor immunity and support immune evasion and tumor escape. They exhibit reduced IFN-α production upon TLR9 stimulation and can induce IL-10 producing $CD4^+$ and $CD8^+$ Treg [35,36]. This suggests that anti-tumor immune responses can be regulated through both modulation of pDC function by the tumor and by limiting anti-tumor cytolytic activity through induction of $CD8^+$ Treg.

Concerning the association of Tregs and prognosis, it has been reported that an increased number of circulating Tregs predicts poor survival of patients with renal cell carcinoma [4], gastric and esophageal cancers [7], myelodysplastic syndrome [37] and HCC [11]. In addition, tumor-infiltrating Tregs were associated with reduced survival in ovarian cancer [12] and HCC patients [1]. In addition, we found that $CD45RO^+CD4^+CD25^{high}$ T cell subset was associated with larger tumor burdens, implying that a subset of Tregs may contribute to the promotion of tumor cell growth in the liver. However, it is also well possible that this just reflects stronger activation caused by a larger amount of antigen.

We performed the functional evaluation of Tregs derived from HCC patients by incubating with responder $CD4^+CD25^-$ T cells (Tresp). We observed that $CD45RO^+$ $CD4^+CD25^{high}$ T cells of HCC patients did not suppress the proliferation of responder T cells when co-cultured at Treg/Tresp ratios of 1:2 and 1:8 (data not shown). In contrast, Hoffmann et al. confirmed that the $CD45RA^+$ $CD4^+CD25^{high}$ T cells of healthy volunteers give rise to a homogeneous and highly suppressive Treg cell population, whereas $CD45RA\text{-}CD4^+CD25^{high}$ T cells generate cell lines with mixed phenotype and function [38]. Although the reasons of these conflicting data were not clarified in the current study, cell viability, apoptosis susceptibility, involvement of Th1 cytokines, and interaction to helper T cell subsets of Tregs obtained from HCC patients need to be evaluated in the future experiments.

This study may be helpful for a better characterization of Treg subsets in the peripheral circulation of patients with HCC, which may establish the immunosuppressive environment to promote tumor progression. Furthermore, to gain insights into changes in the Treg subsets

during the therapeutic option may lead to more effective immunotherapies against cancer and may improve prognosis.

Conflict of interest

None declared.

Acknowledgements

We thank Ms. Mariko Katsuda for technical assistance. We also thank the patients for participating in this study.

References

[1] J. Zhou, T. Ding, W. Pan, L.Y. Zhu, L. Li, L. Zheng, Increased intratumoral regulatory T cells are related to intratumoral macrophages and poor prognosis in hepatocellular carcinoma patients, Int. J. Cancer 125 (2009) 1640–1648.
[2] Y. Nakamoto, E. Mizukoshi, H. Tsuji, Y. Sakai, M. Kitahara, K. Arai, T. Yamashita, K. Yokoyama, N. Mukaida, K. Matsushima, O. Matsui, S. Kaneko, Combined therapy of transcatheter hepatic arterial embolization with intratumoral dendritic cell infusion for hepatocellular carcinoma: clinical safety, Clin. Exp. Immunol. 147 (2007) 296–305.
[3] L.A. Ormandy, T. Hillemann, H. Wedemeyer, M.P. Manns, T.F. Greten, F. Korangy, Increased populations of regulatory T cells in peripheral blood of patients with hepatocellular carcinoma, Cancer Res. 65 (2005) 2457–2464.
[4] R.W. Griffiths, E. Elkord, D.E. Gilham, V. Ramani, N. Clarke, P.L. Stern, R.E. Hawkins, Frequency of regulatory T cells in renal cell carcinoma patients and investigation of correlation with survival, Cancer Immunol. Immunother. 56 (2007) 1743–1753.
[5] J. Visser, H.W. Nijman, B.N. Hoogenboom, P. Jager, D. van Baarle, E. Schuuring, W. Abdulahad, F. Miedema, A.G. van der Zee, T. Daemen, Frequencies and role of regulatory T cells in patients with (pre)malignant cervical neoplasia, Clin. Exp. Immunol. 150 (2007) 199–209.
[6] C. Schaefer, G.G. Kim, A. Albers, K. Hoermann, E.N. Myers, T.L. Whiteside, Characteristics of CD4+CD25+ regulatory T cells in the peripheral circulation of patients with head and neck cancer, Br. J. Cancer 92 (2005) 913–920.
[7] K. Kono, H. Kawaida, A. Takahashi, H. Sugai, K. Mimura, N. Miyagawa, H. Omata, H. Fujii, CD4(+)CD25 high regulatory T cells increase with tumor stage in patients with gastric and esophageal cancers, Cancer Immunol. Immunother. 55 (2006) 1064–1071.
[8] L. Strauss, C. Bergmann, W. Gooding, J.T. Johnson, T.L. Whiteside, The frequency and suppressor function of CD4+CD25highFoxp3+ T cells in the circulation of patients with squamous cell carcinoma of the head and neck, Clin. Cancer Res. 13 (2007) 6301–6311.
[9] A.M. Wolf, D. Wolf, M. Steurer, G. Gastl, E. Gunsilius, B. Grubeck-Loebenstein, Increase of regulatory T cells in the peripheral blood of cancer patients, Clin. Cancer Res. 9 (2003) 606–612.
[10] F. Ichihara, K. Kono, A. Takahashi, H. Kawaida, H. Sugai, H. Fujii, Increased populations of regulatory T cells in peripheral blood and tumor-infiltrating lymphocytes in patients with gastric and esophageal cancers, Clin. Cancer Res. 9 (2003) 4404–4408.
[11] J. Fu, D. Xu, Z. Liu, M. Shi, P. Zhao, B. Fu, Z. Zhang, H. Yang, H. Zhang, C. Zhou, J. Yao, L. Jin, H. Wang, Y. Yang, Y.X. Fu, F.S. Wang, Increased regulatory T cells correlate with CD8 T-cell impairment and poor survival in hepatocellular carcinoma patients, Gastroenterology 132 (2007) 2328–2339.
[12] T.J. Curiel, G. Coukos, L. Zou, X. Alvarez, P. Cheng, P. Mottram, M. Evdemon-Hogan, J.R. Conejo-Garcia, L. Zhang, M. Burow, Y. Zhu, S. Wei, I. Kryczek, B. Daniel, A. Gordon, L. Myers, A. Lackner, M.L. Disis, K.L. Knutson, L. Chen, W. Zou, Specific recruitment of regulatory T cells in ovarian carcinoma fosters immune privilege and predicts reduced survival, Nat. Med. 10 (2004) 942–949.
[13] E. Unitt, S.M. Rushbrook, A. Marshall, S. Davies, P. Gibbs, L.S. Morris, N. Coleman, G.J. Alexander, Compromised lymphocytes infiltrate hepatocellular carcinoma: the role of T-regulatory cells, Hepatology 41 (2005) 722–730.
[14] E. Biagi, I. Di Biaso, V. Leoni, G. Gaipa, V. Rossi, C. Bugarin, G. Renoldi, M. Parma, A. Balduzzi, P. Perseghin, A. Biondi, Extracorporeal photochemotherapy is accompanied by increasing levels of circulating CD4+CD25+GITR+Foxp3+CD62L+ functional regulatory T-cells in patients with graft-versus-host disease, Transplantation 84 (2007) 31–39.
[15] J.N. Stoop, R.G. van der Molen, C.C. Baan, L.J. van der Laan, E.J. Kuipers, J.G. Kusters, H.L. Janssen, Regulatory T cells contribute to the impaired immune response in patients with chronic hepatitis B virus infection, Hepatology 41 (2005) 771–778.
[16] R.W. van Olffen, N. Koning, K.P. van Gisbergen, F.M. Wensveen, R.M. Hoek, L. Boon, J. Hamann, R.A. van Lier, M.A. Nolte, GITR triggering induces expansion of both effector and regulatory CD4+ T cells in vivo, J. Immunol. 182 (2009) 7490–7500.
[17] B. Wilde, S. Dolff, X. Cai, C. Specker, J. Becker, M. Totsch, U. Costabel, J. Durig, A. Kribben, J.W. Tervaert, K.W. Schmid, O. Witzke, CD4+CD25+ T-cell populations expressing CD134 and GITR are associated with disease activity in patients with Wegener's granulomatosis, Nephrol. Dial. Transplant 24 (2009) 161–171.
[18] J.S. Ahn, D.K. Krishnadas, B. Agrawal, Dendritic cells partially abrogate the regulatory activity of CD4+CD25+ T cells present in the human peripheral blood, Int. Immunol. 19 (2007) 227–237.
[19] Q. Tang, J.A. Bluestone, Plasmacytoid DCs and T(reg) cells: casual acquaintance or monogamous relationship?, Nat Immunol. 7 (2006) 551–553.
[20] I.E. Dumitriu, D.R. Dunbar, S.E. Howie, T. Sethi, C.D. Gregory, Human dendritic cells produce TGF-beta 1 under the influence of lung carcinoma cells and prime the differentiation of CD4+CD25+Foxp3+ regulatory T cells, J. Immunol. 182 (2009) 2795–2807.
[21] J. Bayry, F. Triebel, S.V. Kaveri, D.F. Tough, Human dendritic cells acquire a semimature phenotype and lymph node homing potential through interaction with CD4+CD25+ regulatory T cells, J. Immunol. 178 (2007) 4184–4193.
[22] S. Hori, T. Nomura, S. Sakaguchi, Control of regulatory T cell development by the transcription factor Foxp3, Science 299 (2003) 1057–1061.
[23] H. Yagi, T. Nomura, K. Nakamura, S. Yamazaki, T. Kitawaki, S. Hori, M. Maeda, M. Onodera, T. Uchiyama, S. Fujii, S. Sakaguchi, Crucial role of FOXP3 in the development and function of human CD25+CD4+ regulatory T cells, Int. Immunol. 16 (2004) 1643–1656.
[24] J.D. Fontenot, M.A. Gavin, A.Y. Rudensky, Foxp3 programs the development and function of CD4+CD25+ regulatory T cells, Nat. Immunol. 4 (2003) 330–336.
[25] C.L. Maynard, L.E. Harrington, K.M. Janowski, J.R. Oliver, C.L. Zindl, A.Y. Rudensky, C.T. Weaver, Regulatory T cells expressing interleukin 10 develop from Foxp3+ and Foxp3-precursor cells in the absence of interleukin 10, Nat. Immunol. 8 (2007) 931–941.
[26] C.M. Freeman, B.C. Chiu, V.R. Stolberg, J. Hu, K. Zeibecoglou, N.W. Lukacs, S.A. Lira, S.L. Kunkel, S.W. Chensue, CCR8 is expressed by antigen-elicited, IL-10-producing CD4+CD25+ T cells, which regulate Th2-mediated granuloma formation in mice, J. Immunol. 174 (2005) 1962–1970.
[27] H.H. Uhlig, J. Coombes, C. Mottet, A. Izcue, C. Thompson, A. Fanger, A. Tannapfel, J.D. Fontenot, F. Ramsdell, F. Powrie, Characterization of Foxp3+CD4+CD25+ and IL-10-secreting CD4+CD25+ T cells during cure of colitis, J. Immunol. 177 (2006) 5852–5860.
[28] A. Wakkach, S. Augier, J.P. Breittmayer, C. Blin-Wakkach, G.F. Carle, Characterization of IL-10-secreting T cells derived from regulatory CD4+CD25+ cells by the TIRC7 surface marker, J. Immunol. 180 (2008) 6054–6063.
[29] M. Torisu, H. Murakami, F. Akbar, H. Matsui, Y. Hiasa, B. Matsuura, M. Onji, Protective role of interleukin-10-producing regulatory dendritic cells against murine autoimmune gastritis, J. Gastroenterol. 43 (2008) 100–107.
[30] M. Bettini, D.A. Vignali, Regulatory T cells and inhibitory cytokines in autoimmunity, Curr. Opin. Immunol. 21 (2009) 612–618.
[31] K.S. Voo, Y.H. Wang, F.R. Santori, C. Boggiano, K. Arima, L. Bover, S. Hanabuchi, J. Khalili, E. Marinova, B. Zheng, D.R. Littman, Y.J. Liu, Identification of IL-17-producing FOXP3+ regulatory T cells in humans, Proc. Natl. Acad. Sci. USA 106 (2009) 4793–4798.
[32] H. Schmitz-Winnenthal, D.H. Pietsch, S. Schimmack, A. Bonertz, F. Udonta, Y. Ge, L. Galindo, S. Specht, C. Volk, K. Zgraggen, M. Koch, M.W. Buchler, J. Weitz, P. Beckhove, Chronic pancreatitis is associated with disease-specific regulatory T-cell responses, Gastroenterology 138 (2010) 1178–1188.
[33] B. Eksteen, J.M. Neuberger, Mechanisms of disease: the evolving understanding of liver allograft rejection, Nat. Clin. Pract. Gastroenterol. Hepatol. 5 (2008) 209–219.
[34] Shiina, K. Kobayashi, T. Kobayashi, Y. Kondo, Y. Ueno, T. Shimosegawa, Dynamics of immature subsets of dendritic cells during antiviral therapy in HLA-A24-positive chronic hepatitis C patients, J. Gastroenterol. 41 (2006) 758–764.